Volume 2 *January, 1932* *Number 1*

PHYSICS

IMPEDANCE CHARACTERISTICS OF LOADED LECHER SYSTEMS

By Lewi Tonks

General Electric Company, Schenectady, New York

(Received October 29, 1931)

Abstract

Simple formulas are developed for the impedance of short lengths of Lecher system terminated by resistances. This impedance is most simply expressible as a multiple of the surge impedance. The variation of impedance with system length is traced and certain simple relationships are found. It is shown that any system of loads across a Lecher system is equivalent to a certain length of system terminated by a certain resistance. The formulas account for Takagishi's double hump phenomenon and this phenomenon is applied to finding the bridge shortening of an actual bridge. A method of calculating resistance from a resonance curve is derived.

With the increasing interest in the investigation and use of short radio waves, the use of parallel conductor systems as resonant circuits and for measuring purposes is of greater and greater importance. The mathematical theory of such conductors is well known and has already found extensive application to transmission line problems. That formulation is not suited to short wave problems, however, mainly because the line resistance is an important factor in power transmission, whereas in short wave work, this factor, as well as the shunt conductance, is negligible when properly designed conductor systems are used. In working over the theory for the purpose of using it for short wave measurements, the present author has arrived at certain interesting results, some of purely academic interest, perhaps, but others having direct practical application. Although some use has already been made of some of these properties of Lecher systems,[1] it seems that no systematic treatment of them has been given.

The starting point of this investigation is the solution of the problem: To find the impedance of a length of Lecher system terminated by a pure resistance. The solution of the fundamental partial differential equations[2]

$$\frac{\partial V}{\partial x} = L\frac{\partial i}{\partial t}, \quad \frac{\partial i}{\partial x} = C\frac{\partial V}{\partial t} \tag{1}$$

[1] See, for instance, A. A. Oswald, Transoceanic Telephone Service—Short Wave Equipment, Trans. A.I.E.E., **49**, 629 (1930).

[2] The absence of minus signs arises from choosing the positive x-direction opposite to custom. See Fig. 1. This was intentional, the object being to avoid sign difficulties which otherwise appear in the final formulation.

which applies to this case is;

$$\left.\begin{aligned} i &= A\left[\left(\frac{Z_0}{R_t}\right)\cos wx \sin \omega t + \sin wx \cos \omega t\right] \\ V &= AZ_0\left[\cos wx \sin \omega t + \left(\frac{Z_0}{R_t}\right)\sin wx \cos \omega t\right] \end{aligned}\right\} \tag{2}$$

where A is an arbitrary constant, $Z_0=(L/C)^{1/2}$ surge impedance, $R_t=$terminal resistance in ohms, $w=\omega(LC)^{1/2}$, $\omega=2\pi\times$frequency, $L=$inductance per cm of Lecher system, $C=$capacitance per cm of Lecher system, and initial conditions are assumed to be such that $i=0$ at $x=0$ when $t=0$. This simplifies the treatment without any sacrifice of generality.

From electromagnetic theory we know that the velocity of wave propagation is

$$v = 1/(LC)^{1/2} \tag{3}$$

whence

$$wx = 2\pi x/\lambda$$

λ being the wave-length on the conductors. If, then, instead of x, we employ a "reduced" length, l, the unit of which is $\lambda/2\pi$, so that

$$l = 2\pi x/\lambda \tag{4}$$

wx can be replaced by l, with resulting simplification. Another simplification comes from adopting the surge impedance, Z_0, as a unit of impedance and by using "reduced" resistance r_t, "reduced" impedance z, and "reduced" reactance ξ, defined by

$$r_t = R_t/Z_0 \tag{5}$$

$$z = Z/Z_0 \tag{6}$$

$$\xi = X/Z_0 \tag{7}$$

respectively.

From (2) it is readily seen that the absolute value of the impedance $|Z|=|V|/|i|$ is

$$|z| = \left(\frac{r_t^2\cos^2 l + \sin^2 l}{r_t^2 \sin^2 l + \cos^2 l}\right)^{1/2} \tag{8}$$

in reduced units, that the phase of V is

$$\phi_V = \tan^{-1}\left[(1/r_t)\tan l\right]$$

and that the phase of i is

$$\phi_i = \tan^{-1}(r_t \tan l).$$

Accordingly V leads i by the angle ϕ where ϕ is given by

$$\tan\phi = \tan(\phi_V - \phi_i) = \xi/r = (\tfrac{1}{2})(1/r_t - r_t)\sin 2l \tag{9}$$

By using the half-angle formulae, (8) becomes

$$|z| = \left[\frac{(r_t^2 + 1) + (r_t^2 - 1)\cos 2l\xi}{(r_t^2 + 1) - (r_t^2 - 1)\cos 2l}\right]^{1/2} \tag{10}$$

and from this and (9) the reduced resistance and reactance are found to be, respectively,

$$r = \frac{2}{(r_t + 1/r_t) - (r_t - 1/r_t)\cos 2l} = \frac{1}{r_t \sin^2 l + (1/r_t)\cos^2 l} \tag{11}$$

$$\xi = \frac{(1/r_t - r_t)\sin 2l}{(r_t + 1/r_t) - (r_t - 1/r_t)\cos 2l} = \frac{(1/r_t - r_t)}{r_t \tan l + (r_t \tan l)^{-1}}. \tag{12}$$

These two equations are the solution of the problem stated, they give the impedance of any length of Lecher system terminated by any pure resistance. They enable us to speak of the impedance of that portion of such a system which lies to the right (in terms of Fig. 1) of an arbitrary point. There are several interesting features in the behavior of this impedance.

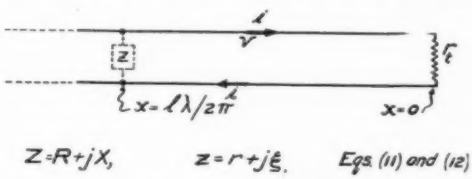

Fig. 1. Impedance equivalent of a length of conductor pair.

If $r_t = 1$ then $\xi = 0$ for all values of l and the impedance of the system is a pure resistance of reduced value unity—the well-known effect of closing a parallel conductor system with a pure resistance equal to the surge impedance.

If any other value of resistance is used, ξ vanishes only when l is a multiple of $\pi/2$, that is, at every quarter wave-length. These points may permissably be called (potential) nodes and loops, a loop occurring at a maximum value of r, a node at a minimum. It can readily be verified that these maximum and minimum values of r are reciprocals of each other, the one being r_t and the other $1/r_t$. This behavior is illustrated in Fig. 2 where the impedance value marked at a point refers to the impedance of the portion of the system below that point.

Another deduction from (11) and (12) is that ξ can be reversed in sign but kept of the same magnitude while r remains unchanged simply by increasing the length of the conductor pair by $(\pi - 2l)$. See Fig. 2. Physically, this means that an inductive reactance at one point becomes an equal capacitive reactance at a point an equal distance on the other side of any node or loop, while the resistance is the same at both places. This relation between the reactances is well known, but the equality of resistance is not so obvious. It can be summed up in the statement that conjugate values of z are symmetrical with respect to nodes and loops.

Of less practical interest, perhaps, is the fact that reciprocal values of z are spaced quarter wave-lengths. The reciprocal values of r at nodes and loops (already noted) is a special case of this.

The conjugate and reciprocal of a given impedance z both have the same phase angle, whence it appears that in the quarter wave-length between a node and its adjacent loop ϕ assumes each value twice. This is shown in Fig.

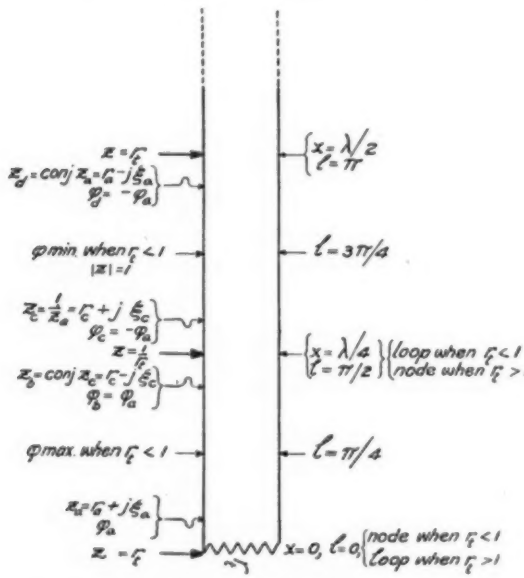

Fig. 2. Impedance relations on a parallel conductor system.

3. Tan ϕ is a harmonic function of l, (x). One notes that at $x = \lambda/8$ and $3\lambda/8$, the absolute value of the impedance is independent of r_t, being equal to the surge impedance of the system.

Having calculated the impedance of a known length of system terminated by a resistance, the converse problem presents itself; that is, to find the length of system and terminal resistance which is equivalent to a known impedance. The elimination of $2l$ between (9) and (10) leads to

$$r_t^4 - r_t^2(z^4 + 1 + (z^2 + 1)^2\xi^2/r^2)/z^2 + 1 = 0 \tag{13}$$

z^2 denoting absolute value, i.e., $z^2 = \xi^2 + r^2$. The two positive roots give the values of resistance which can be used at node or loop respectively. Inspection of the equation shows that the product of these roots is unity, in accordance with what has already been said. Denoting the coefficient of r_t^2 by b, these roots are given by

$$\begin{aligned} r_1, r_2 &= (\tfrac{1}{2})\left[(b+2)^{1/2} \pm (b-2)\right]^{1/2} \\ r_1, r_2 &= (1/2r)(\xi^2 + r^2 + 1 \pm \left[(\xi^2 + r^2 + 1)^2 - 4r^2\right]^{1/2}). \end{aligned} \tag{14}$$

It is readily seen that r_1 and r_2 are always real positive resistances since the radical is necessarily real and less than the other term. If the smaller value,

r_2, is chosen, for the equivalent system, the reduced length of the system is found from (9) to be

$$l = (\tfrac{1}{2}) \sin^{-1} [\xi / r(b-2)^{1/2}] = (\tfrac{1}{2}) \sin^{-1} (\xi / [(\xi^2 + r^2 + 1)^2 - 4r^2]^{1/2}). \quad (15)$$

This equation has two solutions in a half wave-length, but Fig. 3 makes it clear that having chosen r_2 for the equivalent system, l is to be chosen greater

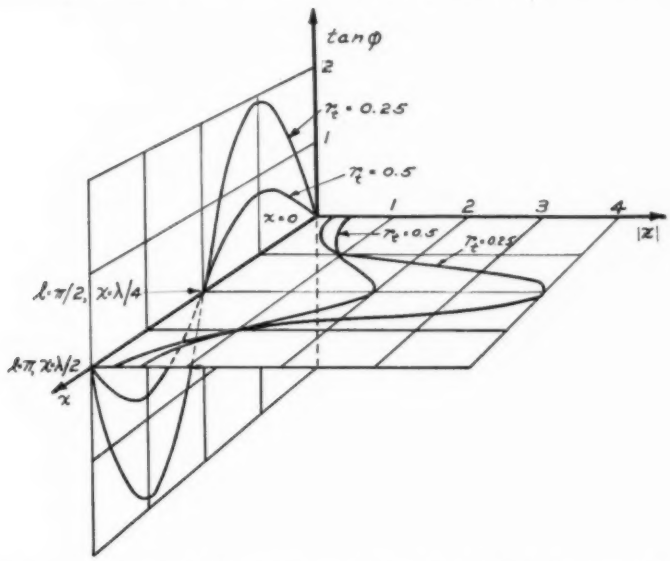

Fig. 3. Impedance of Lecher system as a function of length for two values of terminal resistance r_t.

or less than $\pi/4$ (x greater or less than $\lambda/8$) according as z is greater or less than unity.

We are now in a position to compound loads placed at various points along the system. In the case illustrated in Fig. 4, for instance, the terminal impedance Z_1 can be replaced by the additional length l_1 and resistance r_1 calculated by Eq. (14) and (15). The equivalent system thus extends a distance l_0+l_1 beyond Z_2 and is equivalent to the impedance Z_1' (calculated by (11) and (12)) in parallel with Z_2. Their combined impedance can then be replaced by the equivalent l_{12} and r_{12}. This same procedure is, of course, well known in transmission line problems, with the complication there that complex line lengths are encountered.

Reasoning of this type shows that the use of short-circuiting bridges whose reactance is not zero is justified, since the actual bridge can be replaced conceptually by an ideal (reactanceless) bridge at a fixed[3] small distance beyond it. Eq. (14) shows that the resistance of this ideal bridge is the same as that of the actual bridge to a first approximation if $\xi^2 \ll 1$, $r^2 \ll 1$. These conditions are easily realized in practice.

[3] This distance, known as the "bridge-shortening," is invariable as the bridge is moved and is not sensitive to frequency change as long as its reduced inductance is small, $\xi < < 1$. See (15).

The inactive or free end of a conductor system may easily exhibit resonance in such a way as to confuse measurements. Care in interpretation of results and in the use of very low impedance bridges only is necessary to minimize, but possibly not completely to eliminate this difficulty. A method which obviates the difficulty completely is to use a double instead of a single bridge. The bridge proper, B_1 in Fig. 5, which may be a thermocouple as indicated,

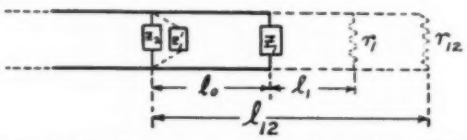

Fig. 4. Compounding of loads distributed along a Lecher system. (The distances as indicated are expressed in reduced units.)

has a low impedance (short-circuiting) auxiliary bridge B_2 attached to it at a fixed distance l. The total reduced impedance ξ_2, across the system at B_2 (B_2 shunted by free end) can never greatly exceed the impedance of B_2, for even if the length of the inactive end is $\lambda/4$, the small resistance which is ever present prevents the building up of a high impedance in the parallel-tuned circuit made up of the inductance in B_2 on the one hand and the effective

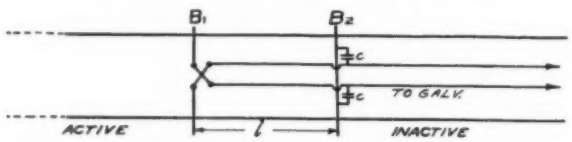

Fig. 5. Design of bridge for eliminating free-end effects.

capacity of the free end on the other. Now l can be chosen so that both ξ_2 and the impedance of B_1 are negligible compared to the impedance arising from l. In this way the most extreme impedance variations in the inactive end are completely cut off from B_1. In addition, the impedance of l can usually be made high enough compared to the impedance of B_2 so that its effect as a shunt is negligible. Numerically on parallel wire systems, Z_0 is usually several hundred ohms. With $l=\lambda/8$ and 3ω in B_1, less than 3 percent of the current escapes B_1 and this is reduced many-fold by increasing l to the neighborhood of $\lambda/4$. (The condensers indicated in the figure prevent high frequency charging currents along the galvanometer leads from affecting the thermocouple reading.)

As a practical example of compounding impedances, the case of double hump resonance discussed by E. Takagishi[4] can be very simply handled. Let the conductor pair P_1, P_2, Fig. 6 form a part of an oscillating circuit and let N

[4] E. Takagishi, On a Double Hump Phenomenon of Current Through a Bridge Across Parallel Lines, Proc. I.R.E. **18,** 513 (1930). The treatment which follows applies to a system "closed" (that is, having a node) at the unexcited end of the active portion, whereas Takagishi deals with the case of an "open" system. The analysis which has already been made shows that the two cases are essentially the same, the "open" end being replaceable by an additional quarter wave-length of "closed" system.

be the position of an ideal ($\xi = 0$) low resistance bridge for which the reactance of the whole circuit vanishes. If now the bridge is shifted to N', resonance can be restored by introducing an inductance L of suitable reduced reactance ξ_L at the proper position designated by q, Fig. 6. We have to find the conditions imposed on ξ_L and q. The reduced impedance of the system at L is by (11) and (12)

$$\begin{aligned} z_{bq} &= r_{bq} + j\xi_{bq} \\ &= \frac{r_t + j(1 - r_t^2)\sin(b+q)\cos(b+q)}{\cos^2(b+q) + r_t^2 \sin^2(b+q)} \end{aligned} \tag{16}$$

which combined with ξ_L gives

$$z_{bqL} = \frac{(r_{bq} + j\xi_{bq})j\xi_L}{r_{bq} + j(\xi_{bq} + \xi_L)} = r_{bqL} + j\xi_{bqL}.$$

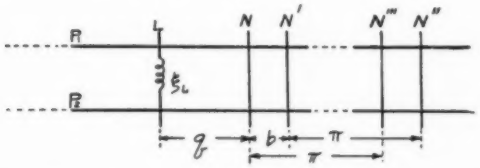

Fig. 6. Analysis of double-hung resonance. (All distances are expressed in reducted units.)

If the system is to be in resonance, ξ_{bqL} must be the same as that with the bridge at N and L absent, that is,

$$\xi_q = \xi_{bqL} = \xi_L \frac{r_{bq}^2 + \xi_{bq}(\xi_{bq} + \xi_L)}{r_{bq}^2 + (\xi_{bq} + \xi_L)^2}. \tag{17}$$

When $\xi_L \gg r_t$, the resistance may be neglected in comparison with reactance and this becomes

$$\xi_q = \xi_L \xi_{bq}/(\xi_L + \xi_{bq}) \tag{18}$$

and since, when $b+q$ is small,

$$\begin{aligned} \xi_{bq} &= \tan(b+q) = (\tan b + \tan q)/(1 - \tan b \tan q) \\ &= (\xi_b + \xi_q)/(1 - \xi_b \xi_q) \end{aligned} \tag{19}$$

(18) becomes

$$(1 - \xi_L \xi_b)\xi_q^2 + \xi_b \xi_q - \xi_L \xi_b = 0. \tag{20}$$

Since this is quadratic in ξ_q, it appears that for given values of b and L there are two positions of L (as fixed by ξ_q) for which resonance occurs. This is the "double hump" phenomenon. Solving (20) we have

$$\xi_{q1}, \xi_{q2} = \frac{-\xi_b \pm (\xi_b^2 + 4\xi_L \xi_b - 4\xi_L^2 \xi_b^2)^{1/2}}{2(1 - \xi_L \xi_b)} \tag{21}$$

for its two roots. In order that approximations which have already been made shall be valid, ξ_{q1} and ξ_{q2} must be small. This requires that $\xi_L\xi_b \ll 1$. If, in addition, b is small and $4\xi_L > \xi_b$, a series expansion gives

$$\xi_{q1},\ \xi_{q2} = \pm\,(\xi_L\xi_b)^{1/2}(1 \mp \tfrac{1}{2}\,(\xi_b/\xi_L)^{1/2} + \xi_b/8\xi_L + \xi_b\xi_L/2) \tag{22}$$

$$\Delta\xi_q = \xi_{q1} - \xi_{q2} = 2(\xi_L\xi_b)^{1/2}(1 + \xi_b/8\xi_L + \xi_b\xi_L/2) \tag{23}$$

and

$$\left.\begin{aligned} \xi_{q1} &= (\Delta\xi_q/2)(1 - \xi_b/\Delta\xi_q) \\ \xi_{q2} &= -\,(\Delta\xi_q/2)(1 + \xi_b/\Delta\xi_q) \end{aligned}\right\}. \tag{24}$$

Since the reduced reactances are small, they can be replaced by the corresponding distances. Eqs. (24) thus give the position of the node in terms of the separation of the resonance positions and the shift in the bridge.

An apparent difficulty is immediately evident in that (23) shows that $\Delta\xi_q/2 > \xi_b$ under the assumed conditions, whence ξ_{q2} is greater than ξ_b in magnitude and the corresponding resonance position of L lies to the right of N'! But a shift of $\pi + b$ (i.e., $\lambda/2 + b\lambda/2\pi$) in N to N'' gives the same impedances to the left of N' as the shift to N' itself. Thus by making the larger shift both resonance positions of L lie on the active side of the bridge and the difficulty vanishes.

It is desirable to know the bridge shortening if inductances and capacities are to be measured by means of a Lecher system. A method based on double hump resonance affords a simpler and more direct method than the usual one of comparing the apparent half wave-length with the apparent full wave-length when the active portion of the system is in each case terminated by the same two similar bridges. By using a bridge which may conveniently carry a thermocouple for measuring the high frequency current, two successive resonance positions of the bridge corresponding to N and N''' in Fig. 6 are found. Then, with the bridge at N'', a small distance beyond N''', an inductance L is placed across the system near N and the two positions of L ($q = q_1$ and $q = q_2$ respectively) for which the current is a maximum, are observed. Eqs. (24) show that to a first approximation the true node at resonance then lies midway between these two positions, since $\xi_q = \tan q = q$ for the small values considered. The bridge shortening is then the distance from this node to the first resonance position of the bridge.

As an example, two resonance positions of a thermocouple bridge were found at 11.75 and 89.4 cm, respectively, on a Lecher system whose calculated surge impedance was 353 ohms. With the bridge at 90.1 cm, a bridging inductance produced resonance when at 12.7 and at 20.15 cm. The true node thus lay at $(12.7 + 20.15)/2 = 16.4$ cm to a first approximation and the bridge shortening is $16.4 - 11.75 = 4.65$ cm. With (24) the first order correction may be applied.[5]

$$q_1 = \frac{20.15 - 12.7}{2}\left(1 - \frac{90.1 - 89.4}{20.15 - 12.7}\right) = 3.35$$

[5] Actual instead of reduced distances can be used here since only ratios are involved.

whence the corrected node lay at $12.7+3.35=16.05$ and the corrected bridge shortening is $16.05-11.75=4.30$ cm. A good estimate of the inductance used can be made with (23). To a first approximation

$$\xi_L = (\Delta\xi_q)^2/4\xi_b = (7.45 \times 2\pi/\lambda)^2/4 \times 0.7 \times 2\pi/\lambda = 19.9 \times 2\pi/\lambda$$

and since $\lambda/2=89.4-11.75=77.65$ cm, the reduced reactance is

$$\xi_L = 19.9 \times \pi/77.65 = 0.80$$

and

$$Z_0\xi_L = 353 \times 0.80 = 282\omega.$$

The frequency being 1.95×10^8 herz, the calculated inductance is

$$L = 282/2\pi \times 1.95 \times 10^8 = 0.23\mu h.$$

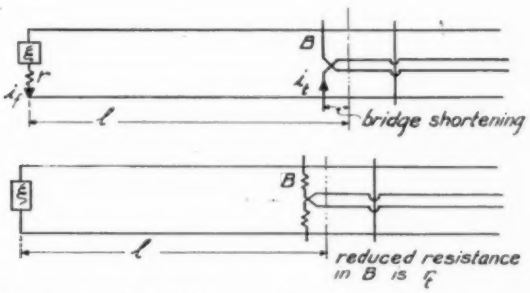

Figs. 7 and 8. Special cases in resistance measurement.

The inductance consisted of a coil which was of 6 turns 0.8 cm long and 0.8 cm in diameter with some additional length of wire and contacts to bridge the 3.9 cm (on center) separation of the conductors. By using a well-known[6] formula, the inductance of the coil alone was found to be 0.20 μh.

Incidentally it is now possible to check the validity of the various assumptions made in dealing with the double hump for the case just cited: (1) $\xi_L \gg r_t$; $Z_0\xi_L=282\omega$ and $Z_0 r_t$ is about 3ω, (2) $\xi_L\xi_b \ll 1$, $\xi_L\xi_b=0.80\times0.7\times2\pi/\lambda=0.023$, (3) $4\xi_L>\xi_b$; these quantities are 3.2 and 0.028 respectively.

The method of measuring inductance and capacity by means of parallel conductor systems is fairly simple and has already been dealt with elsewhere[7] but resistance measurements are more complicated. Two cases will be considered, the one where the resistance is effectively in series with a reactance at the fixed end of the system, Fig. 7, the other in which the resistance is wholly in the movable thermocouple bridge, Fig. 8. In both cases it is assumed that the excitation is a series excitation (not indicated) concentrated at the fixed end of the system. This condition can be approximated to by coupling with the oscillating circuit at this end.

Referring to Fig. 7, the reduced impedance at the fixed end is,

[6] Radio Instruments and Measurements, Bureau of Standards, Circ. No. 74, Eq. (153).

[7] See, for instance, C. R. Englund, The Short Wave Limit of Vacuum Tube Oscillators, Proc. I.R.E. **15**, 914 (1927).

$$z = j \tan l + j\xi + r. \tag{25}$$

If l_r is the value of l at resonance, then

$$j \tan l_r + j\xi = 0$$

whence

$$z = j(\tan l - \tan l_r) + r$$

and, introducing the e.m.f., E;

$$z = j \sec.^2 l_r \delta l + r = E/Z_0 i_f \tag{26}$$

to a first approximation. When l is somewhat less than $\pi/2$, (length $<\lambda/4$) l_r is given with sufficient exactness by the position of B when its current reading i_t is a maximum. Under this same condition (2) shows that

$$i_f = i_t \cos l \tag{27}$$

and combining this with (26)

$$E/Z_0 = i_t \cos l(r + j \sec.^2 l_r \delta l). \tag{28}$$

This is the equation of the resonance curve for small values of δl. Putting the resonance ($\delta l = 0$) value of i_t equal to I_0, and $|i_t| = I_t$ otherwise, (28) gives

$$E/Z_0 = rI_0 \cos l_r = I_t \cos l(r^2 + \sec.^4 l_r \delta l^2)^{1/2}$$

which can be put in the form

$$\delta l/rI_0 \cos^2 l_r = [(\cos l_r/\cos l)^2/I_t^2 - 1/I_0^2]^{1/2}$$

and to the degree of approximation already established,

$$Z_0 \delta l/RI_0 \cos^2 l_r = [1/I_t^2 - 1/I_0^2]^{1/2}.$$

Thus the radical on the right should vary linearly with distance, and if the radical is plotted against distance, the resistance can be found directly from the slope S in amp.$^{-1}$ cm^{-1}. Thus, with (4), it is seen that

$$S = \frac{d[\quad]^{1/2}}{dx} = 2\pi Z_0/\lambda RI_0 \cos^2 (2\pi x_r/\lambda)$$

whence

$$R = 2\pi Z_0/S\lambda I_0 \cos^2 (2\pi x_r/\lambda). \tag{29}$$

Referring to Fig. 8 and by using (11) and (12), the reduced impedance at the fixed end is

$$z = j\xi + j \tan l + r_t/\cos^2 l$$

when $r_t^2 \ll l$ and $\cos l$ is not too small. Proceeding as before

$$z = j \sec.^2 l_r \delta l + r_t/\cos^2 l$$

and

$$r_t I_0/\cos l_r = I_t \cos l(j \sec.^2 l_r \delta l + r_t/\cos^2 l)$$

from which it follows that

$$Z_0 \cos l\delta l/R_t I_0 \cos l_r = [1/I_t^2 - (\cos^2 l_r/\cos^2 l)/I_0^2]^{1/2}$$

or, to the present degree of approximation

$$Z_0\delta l/R_t I_0 = [1/I_t^2 - 1/I_0^2]^{1/2}$$

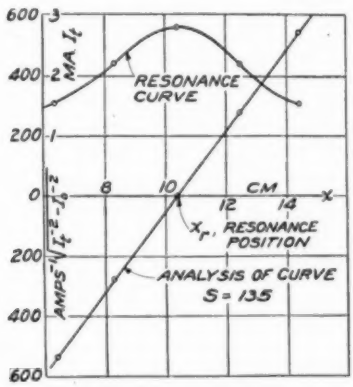

Fig. 9. Resonance curve analysis.

and again the resistance can be found from the slope of the radical—vs.—distance plot;

$$R_t = 2\pi Z_0/S\lambda I_0. \tag{30}$$

A resonance curve thus fails to distinguish between resistance located at the bridge and resistance located at the fixed end of the system and the separation has to be made experimentally. The same reasoning as that just employed shows that with both R_t and R the relation is

$$R \cos^2 (2\pi x_r/\lambda) + R_t = 2\pi Z_0/S\lambda I_0. \tag{31}$$

By replacing R by a short-circuit or low-loss condenser, R_t can be determined first, and then, knowing R_t, R can be found.

Fig. 9 shows the results of applying this formula to the resonance curve obtained when the fixed end of the system was loaded with a high loss condenser. In this case $I_0 = 3.15 \times 10^{-3}$ amp., x_r (corrected for bridge shortening) = 19.6 cm, $\lambda = 154.3$ cm, $Z_0 = 353\omega$. R_t had been determined as 4.9ω. From the figure $S = 135$ amp.$^{-1}$ cm^{-1}. The right hand member of (31) thus has the value 33.7 and $R = 59\omega$.

Finally, it may be remarked that simple relations are to be found on a Lecher system only when the conditions and limits of variation are arranged so that the basic equations, namely, (2), (11), and (12) can themselves be simplified by neglecting certain terms.

PHOTOELECTRIC PROPERTIES OF THIN FILMS OF ALKALI METALS

By S. Asao

Research Laboratory, Tokyo Electric Co.
Kawasaki, Japan

(Received October 29, 1931)

Abstract

Measurements are reported on the color sensitivities of various photoelectric tubes having cathodes made of alkali metals. A composite surface of R-Ag-RO-Ag of any alkali metal R shows a higher sensitivity over a wider range of wave-lengths than R-RO-Ag and has two peaks, one between 330 and 370 mμ, and one at about 500 mμ for potassium and 550 mμ for rubidium and between 700 and 800 mμ for caesium. If a gas filled lamp at 2700°K is used as a light source, photoelectric currents from vacuum photo-tubes are obtained sometimes as large as 29μa per lumen for potassium, and 10–15μa per lumen for rubidium, and 40–50μa per lumen for caesium. It is also reported that the potassium cell in combination with a proper filter would constitute a means for an ideal photometer.

WE REPORTED previously[1] that if a small quantity of silver was evaporated on a caesium oxide photo-sensitive surface, and then the cathode heated again,—the cathode being represented by notation Cs-Ag-CsO-Ag for convenience—the photoelectric sensitivity was enhanced by that additive process.

Later the process was studied systematically for caesium and also applied to potassium and rubidium. The bulbs used in the experiment were made of different materials such as soda glass, a special glass capable of transmitting all radiation of longer wave-length than 300 mμ and fused quartz. The diameter of the bulbs was 6.5 cm and the anode was made of a circular nickel plate of 5 mm diameter. Behind it a tungsten coil holding a silver ball was supported by nickel wires. In making the photo-tube, the bulb was heated at 360°C and then the inner wall was silvered by evaporating the silver ball. The silver layer was then oxidized and a suitable quantity of caesium or other alkali metal was introduced into the bulb from a side tube. The whole bulb was then baked at 150°C, forming a thin film of caesium over the oxidized silver layer. After this, silver was again evaporated and allowed to deposit over the caesium and baked again at 150°C. This final layer of silver had to be very thin. If the silver layer were so thin that the sensitivity was not increased at all, then the process had to be repeated until the maximum sensitivity was attained. If a certain optimum value of silvering was passed, it was found that the sensitivity was decreased.

[1] S. Asao and M. Suzuki, Proc. Phys. Math. Soc. Japan, Oct. 1930; Inst. Rad. Eng. April, 1931.

In order to get the color sensitivity curves, two monochromators were used: one, consisting of a glass prism and lenses, was used to cover the range of wave-length 400–1200 mμ, and calibrated against mercury lines up to 1014 mμ. The light source was a tungsten ribbon filament 3 mm in width. The other, consisting of a quartz prism and lenses, was used for the range 300–600 mμ. The General Electric type S-1 mercury lamp was used as the source, but the light from the tungsten electrodes was entirely avoided and the arc was used exclusively.

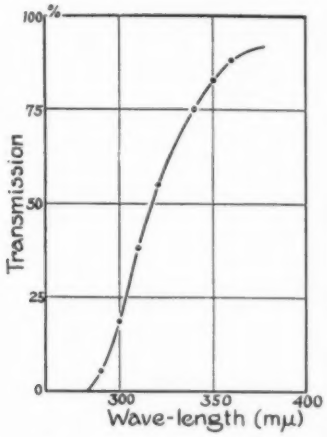

Fig. 1. Transmission curve of soda glass.

Photoelectric currents were measured by means of a galvanometer whose constants were sensitivity, 9.7×10^{-12} amp.; period, 16.4 seconds, and resistance 4270 ohms. The instrument was made by the Institute of Physical and Chemical Research of Japan. The universal shunt for it was made by us. The spectral energy distribution was measured by means of a Leeds and Northrup galvanometer having a sensitivity of 2.5×10^{-9} amp., and coil resistance 13 ohms, and an Adam Hilger thermopile. During the study of shorter wave-lengths, that is, in the case with the S-1 lamp as a source, the spectral energies and photoelectric currents were measured at the same time. This was done by passing the monochromatic light into the photo-tube through the receiving plates of the thermopile. On the other hand, for the longer wave-lengths, the spectral energies from the tungsten lamp were measured before and after the series of experiments. Spectral response characteristics of all photo-tubes were thus plotted by combining the two observations, one covering 400–1200 mμ, the other 297–578 mμ.

Absorption coefficients of the soda glass for one sample were measured in the ultraviolet region as shown in Fig. 1. The observed values were corrected for the absorption of the glass by assuming that the absorption coefficients of all the bulbs made of the same material were the same. This might be allowed in this work because the irregularity of the thickness of the bulb does not cause so much error. Sometimes quartz bulbs were used, and in that case no correction was applied.

Potassium and rubidium as a cathode material were not as thoroughly investigated by the author as caesium. However, they are reported here for a few important facts.

Potassium

After silvering the inner wall of the bulb the silver was oxidized and a suitable amount of potassium was introduced. Then the bulb was heated at a temperature of about 150°C. Potassium tubes were thus made whose char-

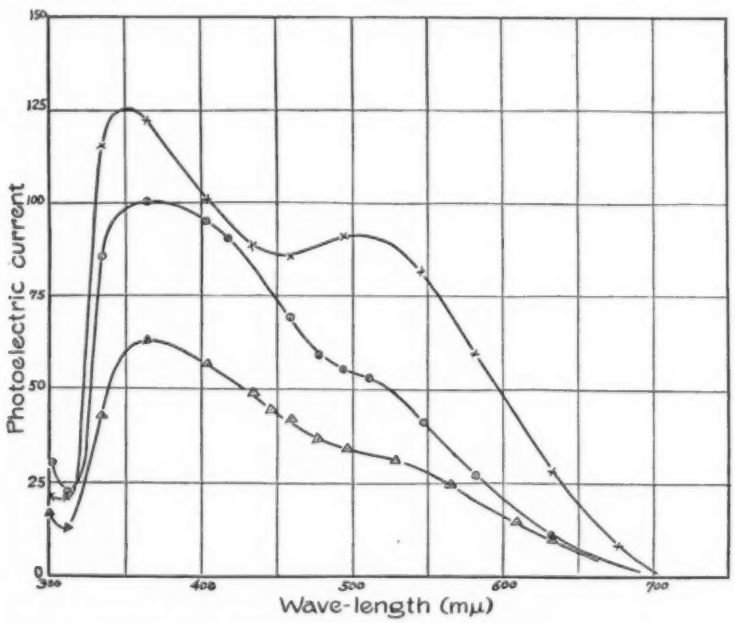

Fig. 2. Colour sensitivity characteristics of K–KO–Ag constant energy.

acteristics are shown in Fig. 2. All have a maximum at about 360 mμ, and another at about 500 mμ, and their sensitivities lie between 3 and 5 μa per lumen. Here, the form of the curves in the range of the longer wave-lengths to the right of 560 mμ is very similar to the right half of the visibility curve as shown in Fig. 3. By obtaining a suitable filter to complete the other half of the curve, such as "Corning Signal Yellow No. 330," (Fig. 4) it is possible to construct a system of the photo-tube and filter whose characteristic nearly coincides with the visibility curve of the eye as shown in Fig. 5. We suggest that this would be a most suitable method for photometry. These thin film vacuum tubes are very constant in photoelectric current and have a long life. A tube which shows change of two percent in photoelectric current is considered to be bad.

The second evaporation of silver over the potassium oxide was then tried and then it was heated as usual. Two curves are shown as in Fig. 6. Both of them have a peak at about 350 mμ. One shows displacement of the long wave limit to 930 mμ, giving 29 μa per lumen, the light source being a gas filled

lamp at 2700°K. The other shows a peak at 530 mμ, giving a sensitivity of 4 μa.

Rubidium

First rubidium vapor from a side tube was deposited spontaneously on the silver layer to form a very thin film. When maximum emission due to the

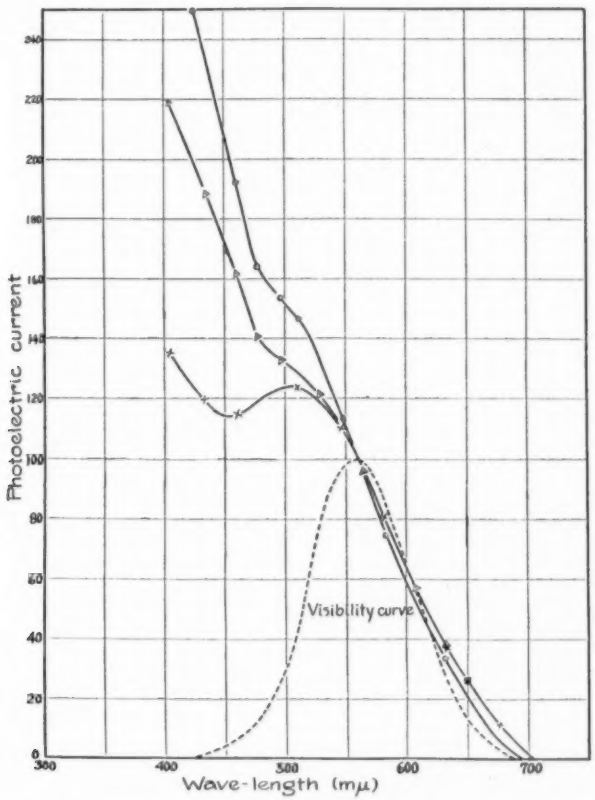

Fig. 3. Colour sensitivity characteristics of K–KO–Ag. The three curves in Fig. 2 are reproduced by making the ordinates at 560 mμ equal.

source of light was gained, the bulb was sealed off and its characteristic curve having a maximum at about 340 mμ was obtained as shown in Fig. 7. In this case gas evolved at sealing off influenced the sensitivity of the photo-tube a little. The behavior of such thin films has been studied by H. Ives.[2] Here this curve was plotted for purpose of comparison with rubidium oxide tube.

Characteristics of a Rb-RbO-Ag and a Rb-Ag-RbO-Ag cathode are shown in Fig. 8. Both have a maximum at about 350 mμ. The Rb-RbO-Ag cathode has another peak at 500 mμ, while the Rb-Ag-RbO-Ag cathode has it at 550 mμ.

[2] H. Ives, Astrophys. J. **60,** 209 (1924).

Caesium

As in the case of rubidium, caesium was deposited spontaneously on the pure silver layer and a Cs-Ag tube was obtained. Its characteristic resembles rubidium and the maximum lies at about 330 mμ as shown in Fig. 9.

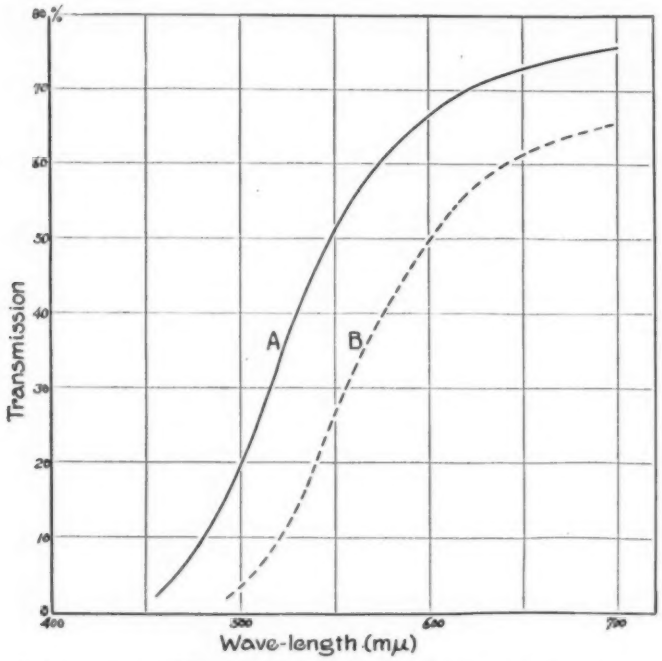

Fig. 4. Transmission curve of "Corning Signal Yellow No. 330." Curve *A*; thickness 1.9 mm; Curve *B*; thickness 4.95 mm.

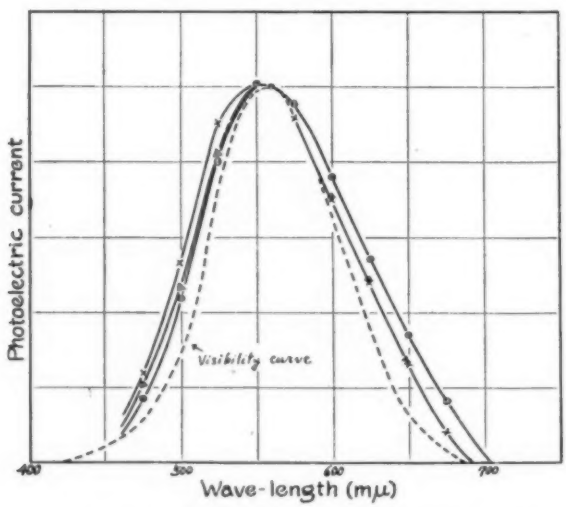

Fig. 5. Colour sensitivity curves obtained by applying the combination of K–KO–Ag and "Corning Signal Yellow No. 330."

The curves of two samples of Cs-CsO-Ag were shown in Fig. 10. Tube No. 1 has an emission of 24 μa per lumen tested with a gas filled lamp at 2700°K. The first peak lies at about 360 mμ, and the second at 750 mμ, agreeing

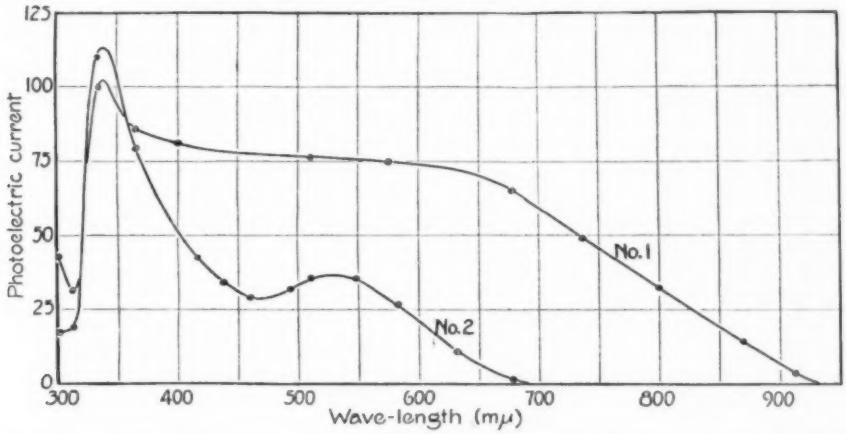

Fig. 6. Colour sensitivity characteristics of K–Ag–KO–Ag constant energy. Curve No. 1, 29 μa per lumen; Curve No. 2, 4 μa per lumen.

closely with that reported by others.[3] Another sample No. 2 is in a quartz tube and has a maximum at about 340 mμ, but no second peak.

Photo-tubes having Cs-Ag-CsO-Ag cathodes had a peak at a longer wave-

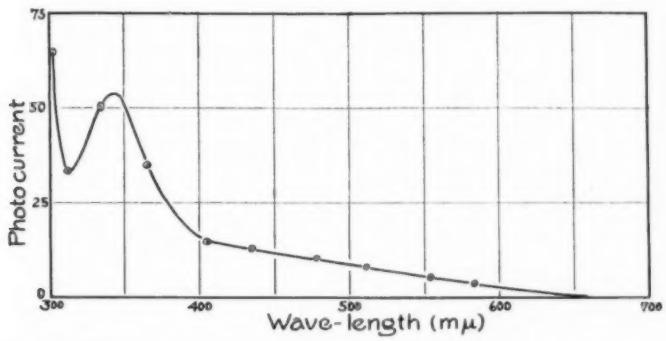

Fig. 7. Colour sensitivity characteristic of Rb–Ag constant energy.

length than Cs-CsO-Ag and the long wave limit extends over to 1200 mμ as shown in Fig. 11. The position of the second peak depended on the relative quantity of oxygen and caesium. Even in the same bulb, the emissions from various parts are not the same but have distinct characteristics. Two curves denoted by No. 2 show emissions from two different parts of the same bulb. The lower curve of No. 2 shows the emission characteristic due to the half of the cathode surface having a uniform color, while the upper curve of No. 2 is that due to the other half having the appearances of patches of various

[3] L. R. Koller, J.O.S.A. **19,** 135 (1929); A. R. Olphin, Phys. Rev. **36,** 251 (1930).

colors. If they are expressed in μa per lumen, the former gives 49 μa, and the latter about 60 μa. The second peak of the lower curves lies at 700 mμ while the upper curve has two maxima in the long wave region, one at about 600 mμ and the other at 800 mμ.

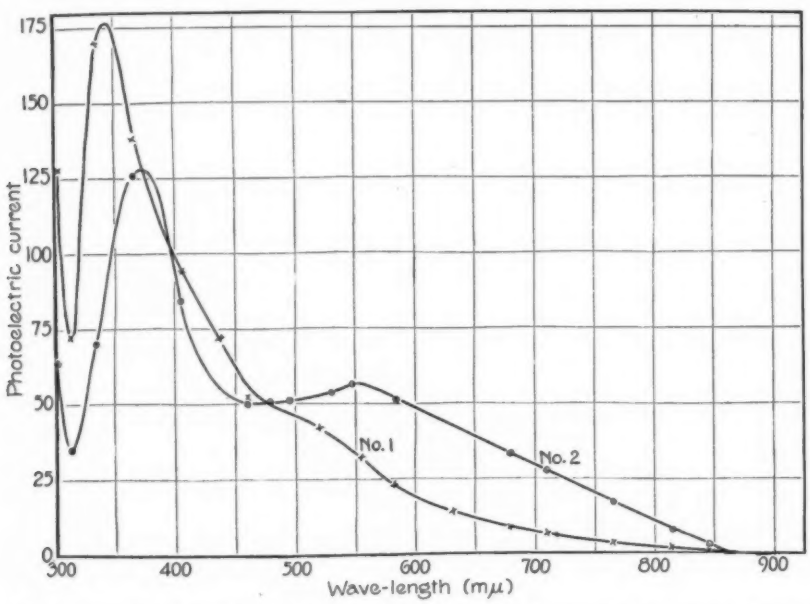

Fig. 8. Colour sensitivity characteristics of Rb–Ag–RbO–Ag constant energy. Curve No. 1, Rb–RbO–Ag; Curve No. 2, Rb–Ag–RbO–Ag.

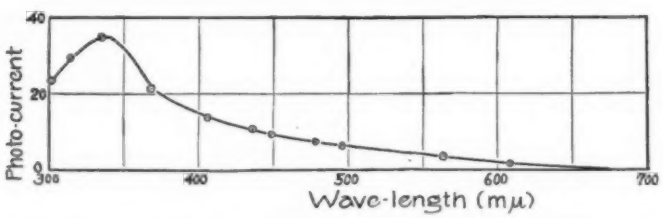

Fig. 9. Colour sensitivity characteristics of Cs–Ag constant energy.

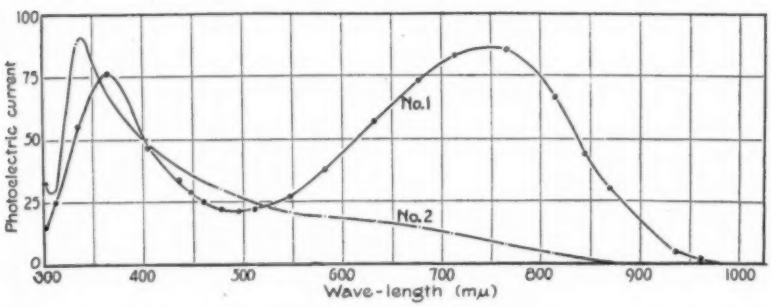

Fig. 10. Colour sensitivity characteristics of C–CsO–Ag constant energy. No. 1, 24 μa per lumen; No. 2, 6 μa per lumen.

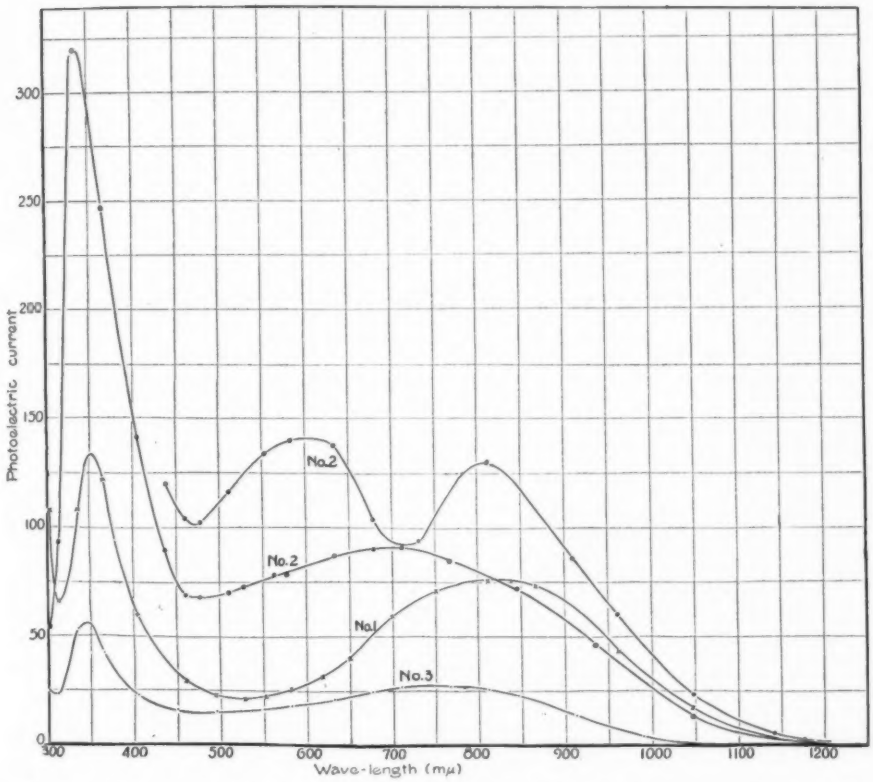

Fig. 11. Colour sensitivity characteristics of Cs–Ag–CsO–Ag constant energy. No. 1, Representative curve of Cs–Ag–CsO–Ag having high emission; No. 2, Two curves referring to different portions of the same bulb. Upper curve corresponds to the sensitivity of 60 μa per lumen, lower curve 49 μa per lumen; No. 3, Less sensitive tube (quartz bulb).

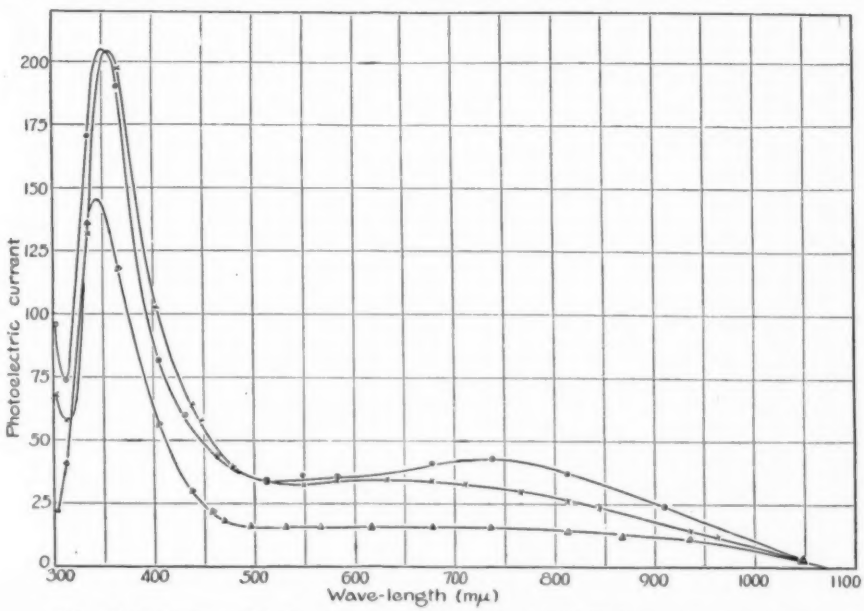

Fig. 12. Colour sensitivity characteristic of Cs–Ag–CsO–Ag constant energy.

When instead of oxidizing the basic layer of silver with oxygen, and then admitting the caesium to make a cathode of the form Cs-Ag-CsO-Ag, caesium was deposited on the silver first and then oxygen admitted into the bulb, we obtained the photo tube having characteristics as shown in Fig. 12. This tube shows a maximum at 700 mμ and a sensitivity of 41 μa per lumen. A peak at shorter wave-length lies at about 330 mμ.

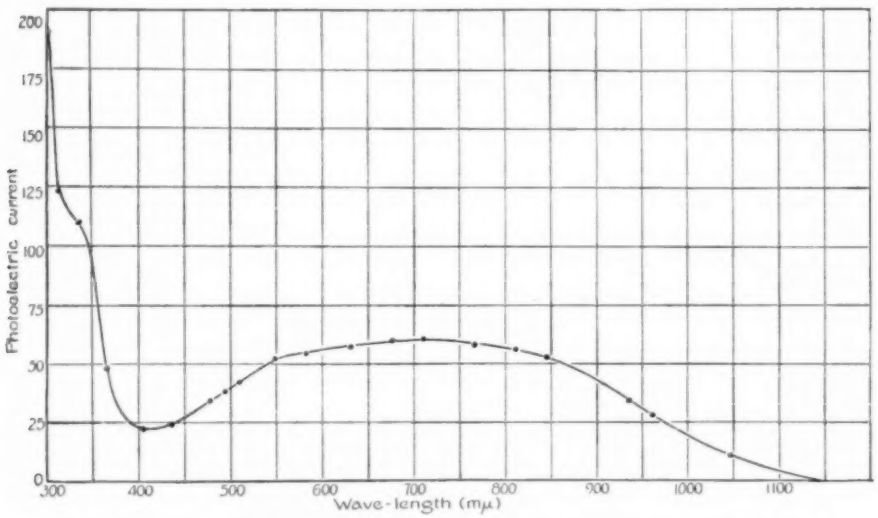

Fig. 13. Colour sensitivity characteristics of Cs–Ag–CsO–Ag constant energy.

If a larger quantity of caesium was introduced on the silver oxide and the excess caesium was absorbed by aquadag in baking the bulb, the resultant caesium oxide surface showed in some cases a deep silvery color, while in others dark brown, and the aquadag took on a red color. After the second thin film of silver was applied to the cathode, the characteristic curves were tested as shown in Fig. 13. These had only a trace of a hump in the long wave region. Peaks at shorter wave-lengths came at about 350 mμ and the tubes showed very high sensitivity.

Acknowledgment

The author sincerely acknowledges the kindness of Dr. M. So for his continual encouragement, Mr. M. Nagashima for making the tubes, and Mr. Y. Hata for assisting in these experiments.

ELECTROKINETIC POTENTIALS. XI. THE EFFECT OF SODIUM SOAPS ON THE ELECTRIC MOMENT OF THE DOUBLE LAYER AT AN AQUEOUS-CELLULOSE INTERFACE*

By Henry B. Bull and Ross Aiken Gortner

Division of Agricultural Biochemistry, University of Minnesota

(Received December 12, 1931)

Abstract

1. Electrokinetic studies of aqueous solutions of sodium formate, sodium acetate, sodium propionate, sodium butyrate, sodium caprylate, sodium oleate and sodium oxalate have been conducted at a cellulose interface with the streaming potential technique.

2. It is suggested that in interest of clearness and accuracy the attempt to express electrokinetic data in terms of "potentials" be abandoned and that the electric moment of the double layer, which does not require a knowledge of the magnitude of the dielectric constant, be substituted for ζ.

3. It is indicated that after the fourth carbon atom has been added the electric moment of the double layer is essentially a constant.

4. It is noted that there is no correspondence between the ionization constant of the fatty acid from which the soap is derived and its effect on the electrokinetic conditions at the interface. This indicates that hydrolysis and the resulting OH ion plays a minor role.

5. It is pointed out that the electric moment of the double layer in the case of the longer chained soaps is almost independent of the concentration whereas that of the short chained soaps are much more sensitive to increased concentration.

6. The maximum electric moment is found at about 2×10^{-4} normal. This is true also for a number of salts.

MARTIN and Gortner,[1] with streaming potential technique, have shown some very interesting relations between molecular structure and the interfacial potentials for the aliphatic alcohols.

Freundlich and Slottman[2] have studied the effect of the following series NH_4Cl, $NH_3(C_2H_5)Cl$, $NH_2(C_2H_5)_2Cl$, $NH(C_2H_5)_3Cl$, and $N(C_2H_5)_4Cl$ on the ζ potential of As_2S_3 with cataphoresis.

It occurred to us that, by using aqueous solutions of the soaps of the fatty acids, a relationship might be found between molecular structure and the electric moment of the double layer. The present paper is a report of such a study.

Experimental

The streaming potential technique was used for determining the electric moment. This method has been described in detail in the previous papers[3] of

* Paper no. 1066, Journal Series, Minnesota Agricultural Experiment Station.

[1] W. McK. Martin and R. A. Gortner, J. Phys. Chem. **34,** 1509–1539 (1930).

[2] H. Freundlich and G. V. Slottman, Zeits. f. physik. Chem. **129,** 305–20 (1927).

[3] H. B. Bull and R. A. Gortner, J. Phys. Chem. **35,** 309–330 (1931).

this series and consists essentially in forcing a liquid through a diaphragm (cellulose in the present case) and measuring with the aid of a quadrant electrometer the difference of electrical potential at the two ends of the diaphragm. It has been the custom hitherto to calculate from these data together with a knowledge of the specific conductivity, viscosity and dielectric

TABLE I. *Data for sodium formate.*

Concentration	Pressure cm Hg (P)	Streaming Potential in millivolts (H)	H/P
1×10^{-4}	58.0	300.0	5.17
	61.3	310.0	5.06
	61.6	310.0	5.03
	66.0	329.0	4.98
	54.9	273.0	4.97
	67.1	325.0	4.84
			Average $H/P=5.008$
Temperature $=30°$; $\kappa_s=36.5\times10^{-6}$ mhos			
2×10^{-4}	61.6	263.0	4.27
	62.7	256.0	4.08
	60.4	247.0	4.09
	63.7	291.0	4.57
	61.4	281.0	4.58
	59.3	271.0	4.57
			Average $H/P=4.36$
Temperature $=30.4°$; $\kappa_s=47.60\times10^{-6}$ mhos			
4×10^{-4}	51.4	106.0	2.06
	58.5	122.0	2.09
	73.1	133.0	1.82
	59.7	140.0	2.35
	57.3	137.0	2.39
	61.7	144.0	2.33
			Average $H/P=2.173$
Temperature $=27.3°$; $\kappa_s=71.91\times10^{-6}$ mhos			
8×10^{-4}	48.0	50.0	1.04
	60.8	59.0	0.97
	56.8	59.0	1.04
	61.9	69.0	1.11
	59.6	64.0	1.07
	55.7	61.0	1.10
			Average $H/P=1.055$
Temperature $=25.2$; $\kappa_s=111.34\times10^{-6}$ mhos			

constant of the liquid the familiar ζ-potential. This is done with the use of the equation.

$$\zeta = \frac{4\pi\eta\kappa_s H}{\epsilon P} \tag{1}$$

where η is the coefficient of viscosity, κ_s is the specific conductivity of the liquid in the diaphragm, i.e., taking into consideration surface conductivity. H is the difference of potential between the ends of the diaphragm, ϵ is the dielectric constant and P is the hydrostatic pressure. All of these quantities are expressed in electrostatic units. Now in the derivation of this equation the following relation is used

$$\zeta = \frac{4\pi qd}{\epsilon} \tag{2}$$

where q is the charge per unit area of the double layer and d is its thickness. By substituting 2 in 1 we obtain

$$qd = \frac{\eta \kappa_s H}{P} . \tag{3}$$

The product qd (distance×charge) is the moment of the double layer (μ)

TABLE II. *Data for sodium acetate.*

Concentration	Pressure cm Hg(P)	Streaming Potential in millivolts (H)	H/P
1×10^{-4}	51.6	409.0	7.93
	59.6	457.0	7.67
	59.5	440.0	7.39
	61.1	490.0	8.02
	55.4	472.0	8.52
	58.2	461.0	7.92
			Average $H/P = 7.908$
Temperature = 29°; $\kappa_s = 29.41\times10^{-6}$ mhos			
2×10^{-4}	52.8	304.0	5.76
	60.9	330.0	5.42
	58.4	318.0	5.45
	62.3	351.0	5.63
	59.6	354.0	5.94
	57.3	339.0	5.92
			Average $H/P = 5.687$
Temperature = 27.2°; $\kappa_s = 42.02\times10^{-6}$ mhos			
4×10^{-4}	57.1	162.0	2.84
	62.4	188.0	3.01
	59.6	179.0	3.00
	54.9	167.0	3.04
	61.1	187.0	3.06
	58.6	178.0	3.04
			Average $H/P = 2.998$
Temperature = 31.2°; $\kappa_s = 72.97\times10^{-6}$ mhos			
8×10^{-4}	73.4	109.0	1.49
	80.2	116.0	1.45
	68.6	105.0	1.53
	77.5	104.0	1.34
	71.4	97.0	1.36
	67.2	92.0	1.37
			Average $H/P = 1.423$
Temperature = 31.5°; $\kappa_s = 123.07\times10^{-6}$ mhos			

and for reasons which will be pointed out in the discussion is, we believe, a more satisfactory way of expressing electrokinetic data.

The diaphragm material was cellulose. A number of packages of Schleicher and Schüll filter paper number 589 were ground in a ball mill with 95 percent ethyl alcohol to a pulp. The cellulose was then filtered and dried in vacuo at 95° centigrade for 8 hours and stored in sealed glass containers. This cellulose is a part of the same material used by Bull and Gortner in their previous studies.[3,4,5].

The sodium soaps used were the formate, the acetate, the propionate, the butyrate, the caprylate, the oleate and the oxalate. The formate and acetate

[4] H. B. Bull and R. A. Gortner, J. Phys. Chem. **35**, 456–466 (1931).
[5] H. B. Bull and R. A. Gortner, J. Phys. Chem. **35**, 700–721 (1931).

were dried at 100° under reduced pressure (*ca.* 30 mm) for 12 hours. The propionate, butyrate, and caprylate were prepared by titrating the pure acid with 5 N NaOH to the neutral point using phenolphthalein as the indicator.

TABLE III. *Data for sodium propionate.*

Concentration	Pressure cm Hg(P)	Streaming Potential in millivolts (H)	H/P
0.4×10^{-4}	53.8	595.0	11.01
	51.7	389.0	11.39
	60.6	631.0	10.41
	52.8	590.0	11.17
	50.7	556.0	10.97
	58.6	651.0	11.11
			Average $H/P=11.010$
Temperature = 29.2°; $\kappa_0 = 18.06\times10^{-6}$ mhos			
1×10^{-4}	48.1	335.0	6.96
	50.2	355.0	7.07
	48.3	344.0	7.12
	51.2	355.0	6.93
	49.2	357.0	7.26
	47.3	338.0	7.15
			Average $H/P=$ 7.081
Temperature = 29.5°; $\kappa_0 = 29.35\times10^{-6}$ mhos			
2×10^{-4}	48.8	246.0	5.04
	47.0	236.0	5.02
	55.7	270.0	4.85
	47.9	230.0	4.80
	56.7	279.0	4.92
	54.6	279.0	5.10
			Average $H/P=4.955$
Temperature = 27.3°; $\kappa_0 = 41.07\times10^{-6}$ mhos			
4×10^{-4}	70.9	196.0	2.76
	77.9	188.0	2.41
	65.1	184.0	2.83
	69.4	186.0	2.68
	66.5	176.0	2.65
	63.9	169.0	2.64
			Average $H/P=2.662$
Temperature = 26.5°; $\kappa_0 = 64.71\times10^{-6}$ mhos			
8×10^{-4}	55.9	86.0	1.54
	50.2	81.0	1.61
	62.3	95.0	1.52
	54.9	73.0	1.33
	63.7	83.0	1.30
	61.1	80.0	1.31
			Average $H/P=1.435$
Temperature = 27.4°; $\kappa_0 = 109.34\times10^{-6}$ mhos			

The soaps were then evaporated to dryness and thoroughly dried at 100° under reduced pressure (*ca.* 30 mm). They were then washed three times with absolute alcohol, dried and the solutions prepared. The oleate was obtained as such. It was purified by four crystallizations from absolute ethyl alcohol. The sodium oxalate was of analytical purity. No additional purification was attempted.

Exact temperature control was not attempted. The temperature at which the experiment was conducted is indicated. In the calculations of the electric moment the value of the viscosity at the particular temperature is substituted

in the equation. For the calculation of the ζ-potential the dielectric constant is also corrected for changes in the temperature. The viscosities used were those for pure water. The data for the viscosity of water in The International Critical Tables were plotted and the value for the particular temperature interpolated from the curve. The dielectric constant was assumed to be equal to that for pure water. It was calculated by use of Drudes' formula.[6]

TABLE IV. *Data for sodium butyrate.*

Concentration	Pressure cm Hg(P)	Streaming potential in millivolts (H)	H/P
1×10^{-4}	54.8	263.0	4.80
	52.7	263.0	4.99
	50.6	253.0	5.00
	53.8	284.0	5.28
	51.7	275.0	5.32
	49.5	266.0	5.37
			Average $H/P=5.127$
Temperature $=27.6°$; $\kappa_s=22.61\times10^{-6}$ mhos			
2×10^{-4}	55.8	213.0	3.82
	55.0	209.0	3.80
	52.7	207.0	3.93
	54.6	202.0	3.70
	54.0	202.0	3.74
	56.1	204.0	3.64
			Average $H/P=3.771$
Temperature $=29.0°$; $\kappa_s=35.26\times10^{-6}$ mhos			
4×10^{-4}	58.7	132.0	2.25
	54.8	128.0	2.34
	52.5	125.0	2.38
	57.4	132.0	2.30
	52.6	123.0	2.34
	58.6	136.0	2.32
			Average $H/P=2.322$
Temperature $=29.0°$; $\kappa_s=57.09\times10^{-6}$ mhos			
7×10^{-4}	53.4	74.0	1.39
	61.6	86.0	1.40
	59.0	84.0	1.42
	52.3	71.0	1.36
	60.4	83.0	1.37
	57.8	80.0	1.38
			Average $H/P=1.387$
Temperature $=31.2°$; $\kappa_s=90.14\times10^{-6}$ mhos			

The conductivity of the solution was determined in the diaphragm in the usual manner, i.e., the resistance was determined with a Leeds and Northrup alternating current galvanometer and the cell constant with N/10 KCl from the Kohlrausch values. Headphones tuned to 1000 cycles vibrations were used to determine the cell constant.

Before attempting a measurement of the potential the cellulose diaphragm was washed out with 250 cc of the solution to be used and allowed to remain in contact with this solution for at least 7 hours. This solution was then replaced by a fresh portion and the determination made. The data reported in the summary and the values used in plotting the curves are the average of

[6] P. Drude, Ann. d. physik. Chem. **59**, 17–62 (1896).

six measurements,—three while streaming the liquid in one direction and three in the reverse. All data are reported. There has been no selection.

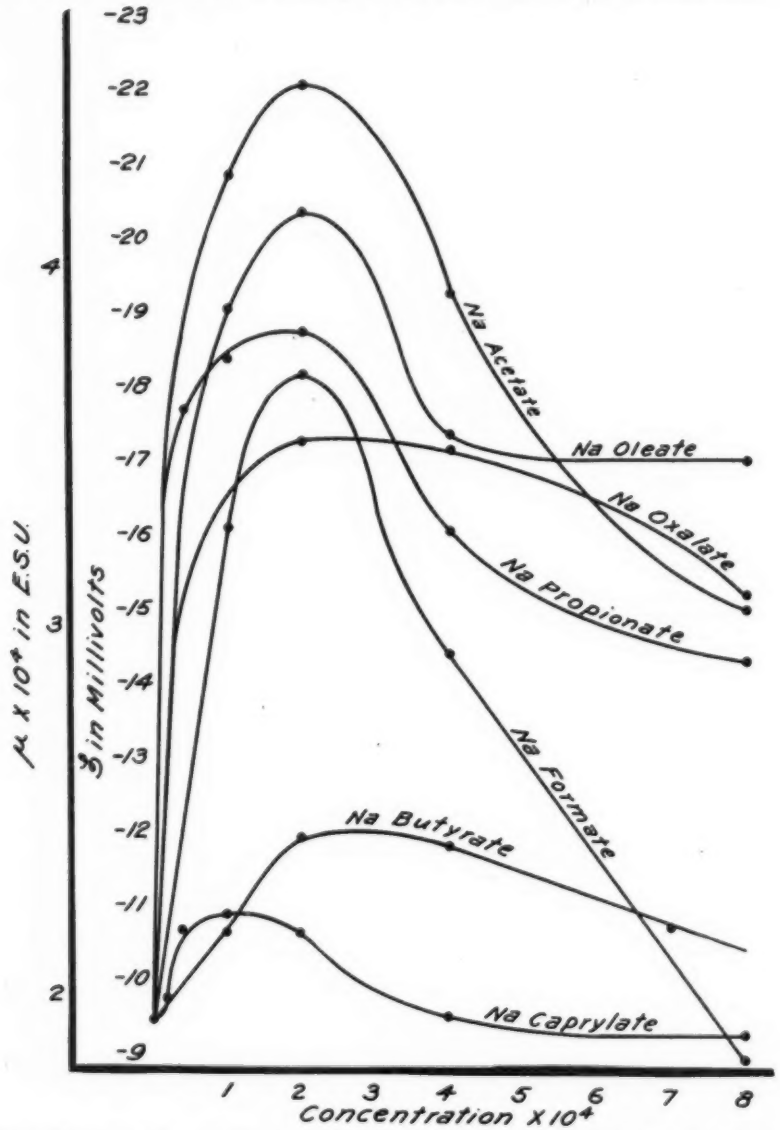

Fig. 1. The electric moment per cm² of the double layer (and the calculated electrokinetic potential) at cellulose-aqueous solution interfaces, as determined by streaming potential technic.

Results

The results of the electrokinetic studies of the aqueous solutions of sodium formate, sodium acetate, sodium propionate, sodium butyrate, sodium caprylate, sodium oxalate and sodium oleate on cellulose are given in Tables I through Table VII and summarized in Table VIII and shown graphically in Figs. 1 and 2.

Discussion

In order to calculate the familiar electrokinetic potential, ζ, which is presumed to be the potential existing across the adsorbed layer of molecules or ions to the movable outer layer it is necessary to know the dielectric constant. It has been the custom to assume that the dielectric constant of the

Table V. *Data for sodium caprylate.*

Concentration	Pressure cm Hg(P)	Streaming potential in millivolts (H)	H/P
0.2×10^{-4}	59.5	532.0	8.94
	71.3	632.0	8.86
	71.0	610.0	8.59
	55.9	510.0	9.12
	72.7	613.0	8.43
	58.7	511.0	8.56
			Average $H/P=8.750$
Temperature $=24.6°$; $\kappa_s=11.49\times10^{-6}$ mhos			
0.4×10^{-4}	61.6	538.0	8.73
	66.1	547.0	8.28
	64.1	549.0	8.56
	60.3	510.0	8.46
	68.1	518.0	7.61
	68.5	524.0	7.65
			Average $H/P=8.220$
Temperature $=25.5°$; $\kappa_s=13.64\times10^{-6}$ mhos			
1×10^{-4}	53.5	274.0	5.12
	50.5	268.0	5.31
	48.5	251.0	5.18
	51.5	306.0	5.94
	49.4	294.0	5.95
	47.5	289.0	6.08
			Average $H/P=5.597$
Temperature $=25.0°$; $\kappa_s=20.16\times10^{-6}$ mhos			
2×10^{-4}	55.1	209.0	3.79
	52.3	201.0	3.84
	49.8	196.0	3.94
	58.7	177.0	3.02
	50.7	157.0	3.10
	48.9	152.0	3.11
			Average $H/P=3.466$
Temperature $=24.0°$; $\kappa_s=30.62\times10^{-6}$ mhos			
4×10^{-4}	54.3	116.0	2.14
	58.5	129.0	2.21
	62.5	133.0	2.13
	59.9	109.0	1.82
	64.1	114.0	1.78
	61.3	109.0	1.78
			Average $H/P=1.977$
Temperature $=26.0°$; $\kappa_s=50.96\times10^{-6}$ mhos			
8×10^{-4}	57.9	59.0	1.02
	55.7	57.0	1.02
	53.4	56.0	1.05
	57.2	66.0	1.15
	54.5	65.0	1.19
	52.4	64.0	1.22
			Average $H/P=1.108$
Temperature $=25.0°$; $\kappa_s=87.20\times10^{-6}$ mhos			

material between the double layers is equal to that of the liquid in bulk. This seems improbable for the following three reasons:

1. According to the theory of Debye,[7] the total electrical polarizability of a medium, to which the dielectric constant is intimately related, is made up of three terms which are the electron polarizability P_e, the atom polariza-

TABLE VI. *Data for sodium oleate.*

Concentration	Pressure cm Hg(P)	Streaming potential in millivolts (H)	H/P
1×10^{-4}	56.6	307.0	5.42
	60.5	309.0	5.11
	58.0	300.0	5.17
	54.2	290.0	5.35
	59.0	304.0	5.15
	56.6	307.0	5.42
			Average $H/P=5.270$
Temperature $=31.5°$; $\kappa_s=42.08\times10^{-6}$ mhos			
2×10^{-4}	52.4	177.0	3.38
	48.9	169.0	3.46
	56.4	191.0	3.39
	51.2	175.0	3.42
	57.8	193.0	3.34
	55.3	184.0	3.33
			Average $H/P=3.387$
Temperature $=29.5°$; $\kappa_s=67.94\times10^{-6}$ mhos			
4×10^{-4}	50.1	80.0	1.60
	55.7	85.0	1.53
	51.6	80.0	1.55
	58.0	88.0	1.52
	54.6	84.0	1.54
	52.6	82.0	1.56
			Average $H/P=1.550$
Temperature $=28.5°$; $\kappa_s=123.80\times10^{-6}$ mhos			
8×10^{-4}	48.3	44.0	.911
	58.7	48.0	.818
	56.4	49.0	.869
	60.2	48.0	.797
	57.5	47.0	.817
	55.4	44.0	.794
			Average $H/P=$ .8343
Temperature $=28°$; $\kappa_s=226.25\times10^{-6}$ mhos			

bility P_a and the orientation polarizability $P\mu$. With substances of high dielectric constant the molecules are always found to possess a large permanent dipole moment. The orientation polarizability may contribute by far the largest proportion towards the dielectric constant. Now at the surface we usually have a tendency for the molecules to become orientated which would certainly increase the dielectric constant above that in the bulk of the liquid.

2. Tarassoff,[8] in a study of the effect of the dielectric constant on the adsorption of gases by charcoal and of a series of pure liquids by fuller's earth has shown that those substances which have a high dielectric constant are preferentially adsorbed and accordingly that a substance with a high

[7] P. Debye, Polar Molecules, page 118, The Chemical Catalog Company, Inc. (1929).
[8] W. Tarassoff, Phys. Zeits. **25**, 369–374 (1924).

dielectric constant will displace another, with a lower dielectric constant, from the interface.

This tendency for the material with a higher dielectric constant to be adsorbed in the electrical double layer in preference to that of lower dielectric

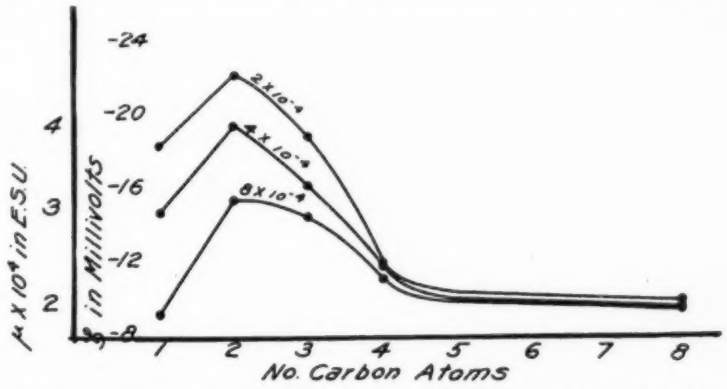

Fig. 2. The electric moment per cm² of the double layer (and the calculated electrokinetic potential) at a cellulose-aqueous solution interface as affected by the number of carbon atoms in a homologous series of the *n*-fatty acid anions. The effect of the concentration of the aqeuous solution is also shown.

constant is a necessary consequence since thereby the electrical potential (ζ) is reduced. This factor is particularly important in the case of a great many organic liquids whose dielectric constant is small because traces of

TABLE VII. *Data for sodium oxalate.*

Concentration	Pressure cm Hg(P)	Streaming potential in millivolts (H)	H/P
2×10^{-4}	57.7	217.0	3.76
	59.8	226.0	3.78
	57.5	219.0	3.81
	56.7	223.0	3.93
	58.7	231.0	3.94
	56.4	218.0	3.87
			Average $H/P=3.848$
Temperature = 34.5°; $\kappa_s = 54.94\times10^{-6}$ mhos			
4×10^{-4}	53.8	128.0	2.29
	59.8	137.0	2.29
	57.4	134.0	2.33
	54.7	121.0	2.21
	58.6	131.0	2.24
	56.2	122.0	2.17
			Average $H/P=2.255$
Temperature = 32.0°; $\kappa_s = 89.33\times10^{-6}$ mhos			
8×10^{-4}	53.1	69.0	1.30
	50.8	62.0	1.22
	57.8	72.0	1.25
	51.9	60.0	1.16
	59.0	71.0	1.20
	56.3	67.0	1.19
			Average $H/P=1.220$
Temperature = 32.8°; $\kappa_s = 149.32\times10^{-6}$ mhos			

water, whose dielectric constant is relatively very high, will be adsorbed almost completely at the surface and thus raise the dielectric constant of the double layer and produce effects all out of proportion to the actual concentration of the water which is present. One has also for the same reason to be very careful about interpreting electrokinetic data obtained in aqueous solutions

TABLE VIII. *Summary of data.*

Concentration $\times 10^4$	Dielectric constant	Viscosity in poises	Specific conductance $\times 10^6$ mhos	ζ in millivolts	μ in e.s.u $\times 10^4$
		Sodium Formate			
1.0	77.1	0.0080	46.5	−16.08	3.28
2.0	76.9	0.0079	47.6	−18.11	3.69
4.0	78.0	0.0085	71.91	−14.40	2.98
8.0	78.8	0.0089	111.34	−9.01	1.88
		Sodium Acetate			
1.0	77.4	0.0082	29.41	−20.83	4.27
2.0	78.0	0.0085	42.02	−22.06	4.56
4.0	76.7	0.0080	72.97	−19.23	3.91
8.0	76.6	0.0077	123.07	−15.01	3.04
		Sodium Propionate			
0.4	77.4	0.0081	18.06	−17.69	3.63
1.0	77.3	0.0081	29.35	−18.36	3.76
2.0	78.0	0.0085	41.07	−18.71	3.87
4.0	78.3	0.0086	64.71	−16.07	3.33
8.0	78.0	0.0085	109.34	−14.41	2.98
		Sodium Butyrate			
1.0	77.9	0.0084	22.61	−10.62	2.19
2.0	77.4	0.0082	35.26	−11.90	2.44
4.0	77.4	0.0082	57.09	−11.87	2.44
7.0	76.7	0.0078	90.14	−10.78	2.19
		Sodium Caprylate			
0.2	79.0	0.0090	11.49	−9.73	2.04
0.4	78.7	0.0088	13.64	−10.65	2.22
1.0	78.8	0.0089	20.16	−10.86	2.27
2.0	79.2	0.0092	30.62	−10.61	2.23
4.0	78.5	0.0087	50.96	−9.51	1.98
8.0	78.8	0.0089	87.20	−9.30	1.94
		Sodium Oleate			
1.0	76.6	0.0078	42.08	−19.03	3.86
2.0	77.3	0.0081	67.94	−20.32	4.16
4.0	77.6	0.0083	123.80	−17.31	3.56
8.0	77.8	0.0083	226.25	−17.08	3.52
		Sodium Oxalate			
2	77.5	0.0073	54.94	−17.25	3.45
4	76.4	0.0077	89.33	−17.15	3.47
8	76.1	0.0075	149.32	−15.24	3.07

of organic liquids. It seems almost certain that the dielectric constant in the double layer will be higher than that for the solution in bulk due to preferential adsorption of the water molecules in the double layer.

Furthermore, as Fürth[9] has shown, the dielectric constant of an aqueous solution of sodium chloride is greatly lowered at very low concentration of the solute, ($\epsilon = ca.$ 52 at 0.3% NaCl) and that at higher concentrations the dielectric constant of the solution increases. Accordingly one may expect water

[9] R. Fürth, Phys. Zeits. **25**, 676–679 (1924).

to be preferentially adsorbed from a salt solution into the double layer. Fürth notes that lithium chloride solutions of equivalent concentration have a lower dielectric constant than have sodium chloride solutions and in all of our studies we have found the electrokinetic potentials at interfaces in contact with lithium chloride solutions to be distinctly different from those of similar interfaces in contact with sodium chloride solutions.

3. In the case of aqueous salt solutions we get electrical saturation effects near the ions which materially reduces the dielectric constant.[7] For uni-valent ions this factor is important at ten Angstrom units and becomes increasingly so as we approach the ion. Thus at a distance of four Angstrom units the dielectric constant has been reduced from 80 in bulk to about 15. As the concentration of the solution is increased we increase the importance of the saturation effects in electrokinetics since the thickness of the double layer decreases and probably becomes in the order of magnitude of the distance in which electrical saturation effects are experienced near the ions. This factor tends always to decrease the dielectric constant and make it smaller than that of the liquid in bulk.

We have then at least three factors which tend to change the dielectric constant in the electrical double layer and make it different from that in bulk. The first two which we have discussed tend to increase the dielectric constant and are of importance in electrokinetic work with organic liquids. The third factor tends to decrease the dielectric constant and is probably of importance in aqueous salt solutions. These considerations seem to throw so much doubt on the actual value of the dielectric constant in the double layer that it seems best to us to discontinue its use in the calculation of electrokinetic data and simply to express our results as electrical moment which is the charge per unit area of the double layer multiplied by its thickness. It is possible to calculate the electric moment (per cm^2) of the double layer from cataphoretic and electro-endosmotic as well as from streaming potential data.

If at a later date the true dielectric constant of the liquid in the double layer can be ascertained then the true ζ can be calculated from existing data.

It is interesting to note that Fairbrother and Balkin[10] in their studies on the electro-endosmosis of several organic liquids through glass diaphragms, have found what appears to be a rather fundamental relation between what amounts to the moment of the electrical double layer and the number of molecules per unit area of the interface multiplied by the permanent dipole moment of the molecules.

As a caution it is well to refer to the paper by Bikerman[11] in which he found that the critical potential (ζ) of an As_2S_3 sol was practically the same in nitrobenzene as in acetoacetic ester. He worked on the effect of adding $FeCl_3$, $N(C_3H_7)_4I$, $Cu(C_6H_9O_3)$ and Cu oleate, which perhaps indicates that in this case the dielectric constant has the same value in the double layer as it has in the liquid in bulk.

It is indicated in Fig. 2 that as we increase the length of the carbon chain

[10] F. Fairbrother and M. Balkin, J. Chem. Soc. 389–403 (1931).

[11] J. J. Bikerman, Zeits. f. physik. Chem. **115,** 261–272 (1925).

the individuality of the soaps disappear and we obtain about the same electric moment per cm^2 irrespective of the number of carbon atoms.

We feel that the effects which we have observed are due largely to the carbon chain and not to the OH ions which result from the hydrolysis of the soaps, because there is no correspondence between the behavior of the different soaps and the dissociation constant of the acids[12] from which they are derived.

As we increase the length of the carbon chain the decrease of the electric moment per cm^2 is not nearly so rapid with increasing concentration after the characteristic maximum has been passed. This is progressively shown from sodium formate through sodium caprylate.

In all cases the maximum electric moment per sq. cm occurs at a soap concentration of about 2×10^{-4}. This has been found to be true also for aqueous solutions of NaCl, KCl, K_2CO_3, K_2SO_4, and K_3PO_4 at a cellulose interface as is indicated in earlier papers in this series.

[12] Landolt-Börnstein tables.

MAGNETIC SUSCEPTIBILITY OF SOME BINARY ALLOYS

By Francis L. Meara
Mendenhall Laboratory of Physics

(Received November 9, 1931)

Abstract

The magnetic susceptibilities of eight series of alloys: tin-thallium, antimony-thallium, thallium-cadmium, zinc-cadmium, lead-antimony, tin-antimony, cadmium-antimony and zinc-antimony have been investigated by Gouy's method. In three series,—antimony-cadmium, antimony-zinc and tin-antimony an intermetallic compound is indicated by an abrupt change in the slope of the susceptibility concentration curve. The compounds thus indicated are SnSb, CdSb, and ZnSb with some evidence for the compound Sn_2Tl. There is nearly a linear relation between the susceptibility and the concentration of one of the constituents where the constituents form simple heterogeneous mixtures—a result best illustrated in the zinc-antimony series of alloys.

ALTHOUGH the magnetic susceptibilities of many alloys have been measured, there are still insufficient data to make a proper correlation between the magnetic susceptibilities and other physical properties. The present investigation was undertaken to extend the data in this field and to correlate them whenever possible with the data on thermal and electrical properties of alloys and with the x-ray data on crystal structure.

Experimental Method

The Gouy[1] method for measuring magnetic susceptibilities was used. The specimens were prepared in the form of small cylindrical rods about 8 cm long and 0.35 cm in diameter. They were suspended from one arm of a Sartorious microbalance capable of measuring to one millionth of a gram. However in most cases readings were taken only to one one hundred thousandth of a gram as this gave results well within the experimental error. The specimens were suspended in such a way that when the magnet was energized the lower end of the specimen was located in a uniform magnetic field while the upper end was far enough from the pole pieces to be in a weak but known field. The pole pieces were about 5 cm in diameter and were at a distance of 0.7 cm from each other. The magnetic field was measured by means of a flip coil and a standard mutual inductance. For a current of 9 amperes it was 22179 gauss and was determined with an accuracy of one or two parts in a thousand. Measurements were made at the center of the gap and at a number of different points above the specimen so that the field at end of the specimen was accurately known.

The densities of the alloys were determined by means of the same micro-

[1] Stoner, Magnetism and Atomic Structure, p. 40.

balance used to determine the force due the magnetic field. The specimens were weighed in air and then in distilled water, the temperature of which was known to one tenth of a degree. The water had been recently boiled to remove occluded air. The difference in weight of the specimens in air and in water, usually more than one gram, was determined to five decimal places, with ordinary corrections to reduce weighings to vacuum.

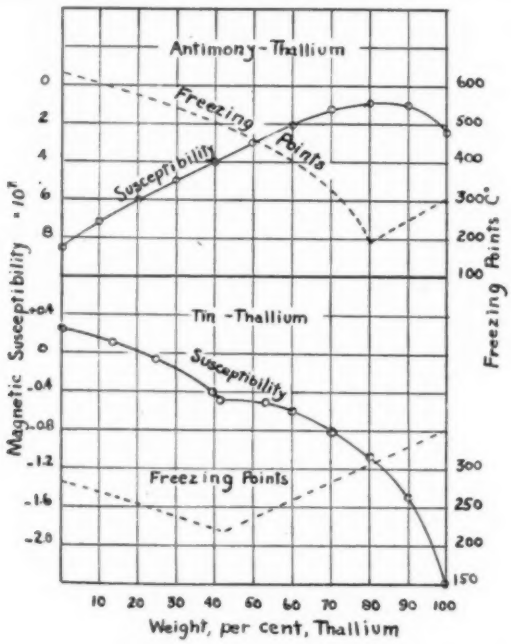

Fig. 1. Magnetic susceptibilities of antimony-thallium and tin-thallium alloys.

The mass susceptibility was calculated from the following formula for a magnetic field of approximately 22,000 gauss

$$\chi = \frac{2F.g}{ad(H_1^2 - H_2^2)}.$$

Where χ = the mass susceptibility, F = the force in grams due to the magnetic field, a = the cross-sectional area of the specimen, d = the density of the specimen, H_1 = the magnetic field at the lower end of the cylindrical rod, and H_2 = the magnetic field at the upper end of the cylindrical rod.

Preparation of Specimens

The specimens were prepared from the purest metals to be obtained. The lead and tin were Kahlbaum's purest metals; thallium, chemically pure metal from Eimer and Amend and the remainder, Baker's analyzed metals.

The constituents of any one alloy were first weighed out in the proper amounts, then put into a Pyrex glass tube connected to a megavac pump, a suitable pressure gauge and a tank of nitrogen of high purity. The tube con-

taining the metals which were to be fused for the alloy, was first evacuated to a pressure of 10^{-3} mm of mercury and then nitrogen was admitted until the pressure was about equal to atmospheric pressure. This process was repeated several times. The metals were then fused. In those cases where the melting point of one of the constituents was above 600°C the nitrogen was allowed to remain in the Pyrex tube at atmospheric pressure. After both metals had been fused and were thoroughly mixed, they were run into a side tube having the dimensions of the desired specimen and allowed to cool slowly. This side tube was then cut off and glass broken from around the specimen.

The accuracy of the measurement of the force, the density, the area of the cross-section and the magnetic fields was such that the error in the final value for the magnetic susceptibility should lie between one half of one percent and one percent.

Results

The susceptibilities of the following series of alloys were measured: antimony-thallium, tin-thallium, zinc-cadmium, lead-antimony, tin-antimony, cadmium-antimony and zinc-antimony.

Tin-thallium.

The curve showing the magnetic susceptibility as a function of the concentration of thallium by weight (Fig. 1) is composed of two curved portions with a sharp cusp at 42 percent by weight of thallium. This cusp corresponds to the eutectic of the freezing curve. This is also the concentration at which the compound Sn_2Tl would be expected provided it existed. The parts of this curve on either side of the cusp, however, are not linear as might be expected for the simplest case of a mechanical mixture of such a compound with one of the constituents.

For purposes of comparison the freezing point curve by Fuchs[2] is included. This curve indicates that thallium and tin form a heterogeneous mixture for all concentrations with some uncertainty about dilute concentrations of tin in thallium and thallium in tin. As previously noted there is a eutectic at a concentration of 42 percent by weight of thallium.

Antimony-thallium.

With the addition of antimony to thallium it is evident from Fig. 1 that the diamagnetic susceptibility of this series of alloys decreases, passes through a minimum at about 20 percent by weight of antimony and then increases steadily up to the large value of antimony. The freezing point curve by Williams[3] shows a eutectic at a concentration of 20 percent by weight of antimony so that the minimum of the susceptibility curve corresponds to the eutectic of the freezing point curve. The freezing point curve indicates that the antimony-thallium alloys are heterogeneous mixtures of crystals for all concentrations. While the curve for magnetic susceptibilities is not linear, a

[2] Fuchs, Zeits. f. anorg. Chem. **107**, 308–12 (1919).
[3] Williams, Zeits. f. anorg. Chem. **50**, 127–132 (1906).

large portion of it, from 25 to 95 percent by weight of antimony is nearly linear as should be expected for such mixtures.

An x-ray analysis of this series of alloys by Persson and Westgren[4] shows that this system contains besides pure thallium and pure antimony two

TABLE I.

Antimony-Thallium Series		Tin-Thallium Series		Zinc-Cadmium Series		Thallium-Cadmium Series	
Weight percent Antimony	Mass susceptibility	Weight percent Thallium	Mass susceptibility	Weight percent Cadmium	Mass susceptibility	Weight percent Thallium	Mass susceptibility
0.00	-0.240×10^{-6}	0.00	$+0.025\times10^{-6}$	0.00	-0.157×10^{-6}	0.00	-0.180×10^{-6}
10.27	0.110	12.50	+0.0045	4.83	0.139	9.82	0.182
20.33	0.096	23.78	−0.0039	12.47	0.102	20.15	0.186
30.35	0.164	31.00	0.0238	22.12	0.107	30.00	0.187
39.37	0.213	38.58	0.0418	30.68	0.109	39.72	0.190
50.17	0.294	41.55	0.0428	42.05	0.114	50.45	0.195
60.51	0.395	52.10	0.0557	49.03	0.114	59.43	0.200
70.13	0.492	59.50	0.0614	59.76	0.121	68.90	0.205
80.11	0.593	69.60	0.0845	70.53	0.122	79.19	0.213
87.38	0.706	80.60	0.1060	80.18	0.131	89.93	0.223
100.00	0.857	90.50	0.1442	92.28	0.158	100.00	0.240
		100.00	0.2400	97.29	0.162		
				100.00	0.180		

Tin-Antimony Series		Lead-Antimony Series		Zinc-Antimony Series		Cadmium-Antimony Series	
Weight percent Antimony	Mass susceptibility	Weight percent Lead	Mass susceptibility	Weight percent Antimony	Mass susceptibility	Weight percent Antimony	Mass susceptibility
0.00	$+0.0250\times10^{-6}$	0.00	-0.8570×10^{-6}	0.00	-0.157×10^{-6}	0.00	-0.180×10^{-6}
10.06	−0.0057	9.77	0.3300	10.00	0.164	10.00	0.209
20.46	0.0341	19.73	0.1588	20.00	0.194	18.91	0.197
29.77	0.0807	30.13	0.0152	29.58	0.211	30.79	0.238
40.96	0.1298	39.70	0.0202	39.46	0.234	39.90	0.225
50.00	0.1676	49.96	0.0124	50.42	0.246	49.60	0.331
60.56	0.1512	60.46	0.0286	59.64	0.252	60.00	0.363
69.81	0.1551	70.16	0.0511	70.18	0.375	69.68	0.402
80.30	0.1298	79.85	0.0789	79.92	0.520	79.94	0.559
85.11	0.0573	91.32	0.0918	100.00	0.857	100.00	0.857
90.03	0.0968	100.00	0.1220				
95.07	0.2500						
97.51	0.4080						

phases. One of these phases with about 7 percent antimony in it, is evidently a solid solution of antimony in β-thallium. The other phase corresponds to the formula Tl_7Sb_2 and has a complicated cubical lattice. Neither the susceptibility curve nor the freezing point curve gives any evidence of the compound Tl_7Sb_2.

Thallium-cadmium.

On the addition of thallium to cadmium the diamagnetic susceptibility of this series of alloys (Figs. 2) increases continuously until pure thallium is

[4] Persson and Westgren, Zeits. f. physik Chem. **136,** 3–4 (1928).

reached. There is no evidence of an abrupt change of curvature in the curve at any concentration. The data on the freezing point curve by Kurnakow and Puschin[5] shows that cadmium is slightly soluble in thallium and thallium slightly soluble in cadmium. The remainder of this series of alloys is a heterogeneous mixture of these saturated solutions. The magnetic susceptibility curve departs from the linear relation to be expected on the basis of a hetero-

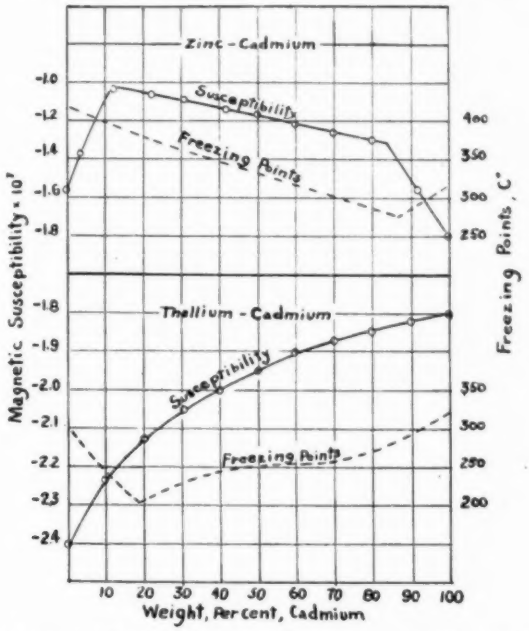

Fig. 2. Magntic susceptibilities of zinc-cadmium and thallium-cadmium alloys.

geneous mixture. There is no suggestion from this curve that thallium is soluble in cadmium but there is some indication from the form of the curve that cadmium is slightly soluble in thallium.

Zinc-cadmium.

The addition of zinc to cadmium (Fig. 2) decreases the diamagnetic susceptibility rapidly until the concentration of cadmium reaches 13 percent by weight. In like manner the addition of zinc to cadmium rapidly decreases the diamagnetic susceptibility until the alloy contains about 10 percent by weight of zinc. Over the intermediate range between these two concentrations the susceptibility is a linear function of the concentration of one of the components in the alloy. This fact indicates that we are dealing with a mechanical mixture, probably of two saturated solid solutions. The freezing point curve by Lorentz and Plumbridge[6] shows a eutectic at 86 percent by weight of cadmium. The concentration at which this eutectic occurs nearly coincides with the concentration at which two linear parts of the susceptibility curves intersect each other.

[5] Kurnakow and Puschin, Zeits. f. anorg. Chem. **30,** 86–108 (1902).

[6] Lorentz and Plumbridge, Zeits. f. anorg. Chem. **83,** 236 (1913).

According to Glasunow and Matweew[7] there is an exact linear relation between the electrical conductivity and the concentration. There thus seems to be a discrepancy between this result and that arrived at from a consideration of the magnetic susceptibility. However since the observations in the two cases were made on series of alloys prepared in somewhat different ways it may be that this lack of agreement arises out of the differences to be attributed to the difference in the physical treatment of the specimens. The

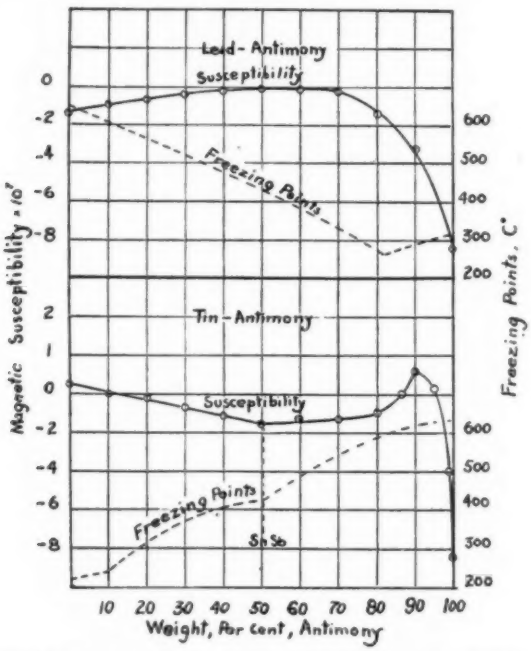

Fig. 3. Magnetic susceptibilities of lead-antimony and tin-antimony alloys.

initial decreases in the diamagnetic susceptibility due to the addition of zinc to cadmium and cadmium to zinc may indicate a solubility of cadmium in zinc and zinc in cadmium over these limited ranges, with mechanical mixtures of these saturated solutions at other concentrations.

This result is in agreement with results obtained by Schaposchinikoff and Sacharov[8] on the hardness and microstructure of the cadmium-zinc alloys. They found that these metals gave no definite compounds and no solid solutions except between 0 and 5 to 7 percent cadmium and between 83 and 100 percent cadmium.

Lead-antimony.

In the lead-antimony series (Fig. 3) the susceptibility decreases with the addition of lead until the alloy contains about 40 percent lead. For higher concentrations of lead there is nearly a linear relation between the sus-

[7] Glasumow and Matweew, Int. Zeits. f. Metallog. **5**, 113–122 (1913).
[8] Schaposchinikoff and Sacharov, Jour. Rus. Phys. Chem. **39**, 907–914 (1907).

ceptibility and the concentration. The electrical conductivity as determined by Matthiessen[9] shows a somewhat analogous departure from a linear relation between conductivity and the concentration of one of the components in the alloy. The magnetic susceptibility of this series of alloys has also been measured by Endo[10] who annealed the specimens for nearly forty hours. This annealing caused the susceptibility to change in such a way that the curve then consisted of two linear portions. The influence of stress on the magnetic susceptibility of pure metals has been observed by Bitter[11] and also by Honda and Shimiziu.[12] Hence it seems probable that internal stresses might decidedly influence the diagmagnetic susceptibility of alloys.

An x-ray analysis of this series of alloys has been made by Solomon and Jones.[13] They found no evidence for definite compounds and also conclude that if antimony is soluble in lead or lead in antimony the degree of solubility of either metal in the other is very small at room temperature This is in agreement with the conclusions to be drawn from the freezing point curve by Gontermann.[14]

Tin-antimony.

In the tin-antimony series (Fig. 3) between 0° and 51 percent by weight of antimony the magnetic susceptibility is a linear function of the concentration, indicating a mechanical mixture over the range. The abrupt change in slope at 51 percent by weight of antimony indicates the existence of the compound SnSb. There is a peculiar rise in the curve between 85 and 95 percent by weight of antimony. This rise is likely caused by crystallization taking place in a definite direction. Leroux[15] found a similar maximum at 92 percent by weight of antimony. These maxima would probably be decidedly changed by more careful annealing. The compound SnSb is also very definitely indicated by the freezing point curve by Williams,[16] by the electrical conductivity and temperature coefficient curves by Konstantinow and Smirnow[17] and by the curve for thermoelectric power.[18]

The x-ray analysis of these alloys by Jones and Bowen[19] established the existence of the compound SnSb. The compound SnSb was found to persist over the range from 40 to 60 percent antimony with some change on the lattice constant showing that both tin and antimony are soluble in it. They also found that the solution of antimony by the compound up to 4 percent causes a change in the lattice constant from 6.092A to 6.106A. Before anneal-

[9] Matthiessen, Pogg. Ann. **110,** 28 (1860).
[10] Endo, Science Rept. Tohoku Imp. Univ. **14,** 1479 (1925).
[11] Bitter; Phys. Rev. **36,** 978–983 (1930).
[12] Honda and Shimiziu, Nature **126,** 990 (1930).
[13] Solomon and Jones, Phil. Mag. **10,** 470 (1930).
[14] Gontermann; Zeits. f. anorg. Chem. **55,** 419 (1907).
[15] Leroux, C. R. **156,** 1764 (1913).
[16] Williams, Zeits. f. anorg. Chem. **55,** 12 (1907).
[17] Konstantinow and Smirnow; Annual Tables of Constants and Numerical Data **2,** 345.
[18] Hutchins; Amer. Jour. of Science **48,** 226 (1894).
[19] Jones and Bowen; Nature **126,** 846 (1930).

ing the solution of 10 percent tin in antimony causes an expansion of the lattice to 6.124A but after annealing there is no measurable change. Internal strains which might be removed by further annealing may explain the maximum at 90 percent antimony and just as annealing removes the change in the dimensions of the crystal lattice so it may be that annealing would remove this peculiarity in the susceptibility.

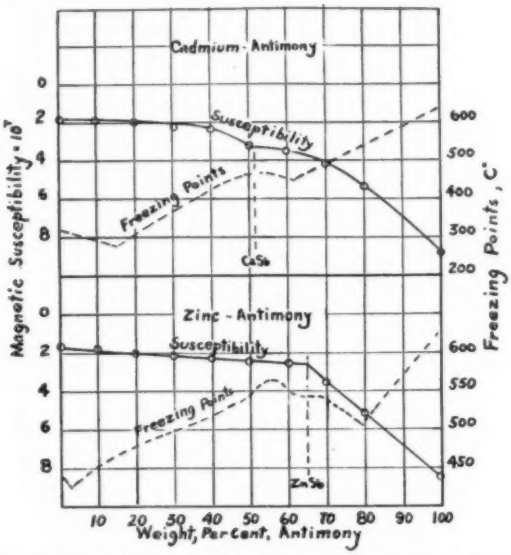

Fig. 4. Magnetic susceptibilities of cadmium-antimony and zinc-antimony alloys.

Cadmium-antimony.

In the cadmium-antimony series of alloys (Fig. 4) the magnetic susceptibility curve shows a sharp cusp at 51 percent by the weight of antimony corresponding to the compound CdSb. From 0 to 40 percent and from 70 percent to 100 percent by weight of antimony the curve for magnetic susceptibilities is nearly linear as might be expected over this range where there is a heterogeneous mixture of the compound CdSb in either antimony or cadmium. The curve for thermoelectric heights,[20] the curve for the Hall constant [21] and the curve for the temperature coefficient of resistance[22] all show exceptionally sharp cusps as the concentration corresponding to the compound CdSb. These curves also show the presence of mechanical mixtures on either side of the concentration at which the compound CdSb is formed. The freezing point curve of Treitschke[23] like the other curves shows the presence of the compound CdSb. A second compound Cd_3Sb_2 may be inferred from some of the results on this series of alloys but Treitschke regards the compound as unstable. The curve for magnetic susceptibilities gives no evidence for the existence of this compound.

[20] Haken, Ann. d. Physik **32,** 291 (1910).
[21] Smith, Phys. Rev. **32,** 178 (1911).
[22] Euken and Gehlhoff; Verh. d. deut. Phys. Ges. p. 169 (1912).
[23] Treitschke, Zeits. anorg. Chem. **50,** 217 (1906).

Zinc-antimony.

The magnetic susceptibility curve for the zinc-antimony series (Fig. 4) is characteristic of a series of alloys in which one intermetallic compound is formed and this compound forms mechanical mixture with both of the pure metals entering into the alloy. This compound is formed where the concentration of zinc is 35 percent by weight. From the concentration at which the compound ZnSb is formed to pure antimony and also from this compound to pure zinc the susceptibility curve is a straight line. This fact indicates that the compound ZnSb forms mechanical mixtures with both zinc and antimony. The freezing point curve by Treitschke,[24] the Hall constant curve by Smith,[25] the thermoelectric height by Haken[26] and the resistivity curve by Eucken and Gehlhoff[27] all definitely indicate the compound ZnSb. The freezing point curve also suggests a second compound Sb_3Zn_2 but this compound is not indicated on the curve for magnetic susceptibilities nor is it indicated on the curves for the Hall constant, the thermoelectric power, or the specific resistance. From this fact it may be inferred that this compound is unstable.

[24] Treitschke, Zeits. f. anorg. Chem. **50,** 217 (1906).
[25] Smith; Phys. Rev. **32,** 178 (1911).
[26] Haken; Ann. d. Physik **32,** 291 (1910).
[27] Eucken and Gehlhoff; Verh. d. deut. Phys. Ges. p. 169 (1912).

A THERMIONIC FREQUENCY DOUBLER

By C. K. Stedman

Physics Department, Purdue University

(Received October 26, 1931)

Abstract

The output voltage e_p of a thermionic tube operated over a suitable restricted range of grid voltages e_g may be represented by the parabola $e_p = b_0 + b_1 e_g + b_2 e_g^2$. By adding to this in opposite phase the output of another tube, operated on the straight line portion of its curve, we may balance out entirely the term $b_1 e_g$, so that the characteristic of the combination of tubes is $e_c = b_0 + b_2 e_g^2$. The system will then operate as a frequency doubler, for the output is proportional to e_g^2 alone. In the experimental set-up described, with a 201A tube, an output of 0.175 volts of frequency $2f$ is obtained from an input of 1.0 volts of frequency f. It is found that when the characteristic of the system is plotted, the curve is never a symmetrical parabola $e_c = b_0 + b_2 e_g^2$ over a very wide range of grid voltages. This is because the coefficient of the cube term in the equation of the tube characteristic is not negligibly small, and the equation must be written $e_c = b_0 + b_2 e_g^2 + b_3 e_g^3$. It is shown how the coefficient b_3 may be determined by measuring the dissymmetry of the curve.

IN THE course of some acoustical research the need has arisen for a frequency doubler which will operate throughout the audible range without serious frequency discrimination, and without the introduction of too many harmonics. The following arrangement has been developed to meet these requirements.

List of Symbols

e_p = Instantaneous value of variable component of plate voltage
i_p = Instantaneous value of variable component of plate current
e_g = Instantaneous value of variable component of grid voltage
e_{gp} = Grid voltage at operating point
e_0 = Output voltage
R_p = a.c. plate resistance
$G_p = 1/R_p$ = a.c. plate conductance
$b_0 b_1$, etc. = Tube constants
$a_0 a_1$, etc. = Tube constants

The ideal thermionic frequency doubler is a circuit whose input voltage-output voltage characteristic is a parabola with vertex at the operating point for all frequencies. For then the output voltage is proportional to the square of the input voltage alone, and contains 100 percent second harmonic. These conditions cannot be met in practice, but it is possible to keep the unwanted harmonics below 5 percent with an output of 0.2 volts at all audio-frequencies.

Consider a tube whose characteristic may be represented by the equation

$$e_{p1} = R_{p1} i_{p1} = R_{p1}(b_0 + b_1 e_g + b_2 e_g^2) \tag{1}$$

over a restricted range about the operating point e_{gp} (the voltages and currents are instantaneous values). The vertex of this parabola is at $e_g = -(b_1/2b_2)$, so it is clear that if we introduce another tube into the circuit to subtract from e_{p1} a voltage proportional to e_g, in a manner to be explained later, and so make $b_1 = -2b_2 e_{gp}$, then the resulting characteristic of the combination is

$$e_{\text{output}} = e_0 = a + R_{p1} b_2 e_g^2 \tag{2}$$

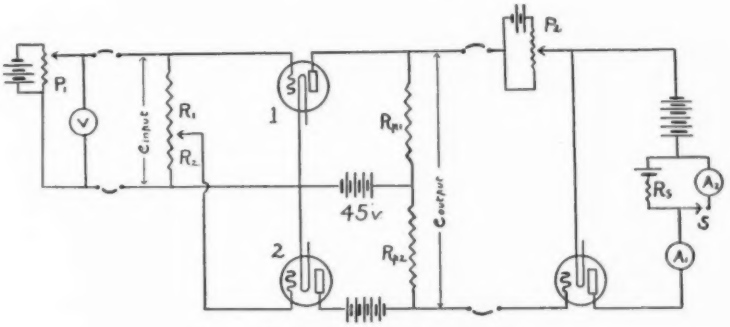

Fig. 1. Frequency doubling circuit.

where e_g is now the grid voltage measured up or down from e_{gp}. If $e_g = E \cos \omega t$, the variable component of the output voltage is $e_v = (R_{p1} b_2/2) E^2 \cos 2\omega t$. Thus a pure sine wave of amplitude E is transformed into one of twice the frequency and amplitude $\frac{1}{2} R_{p1} b_2 E_2$.

Details of the Circuit

The circuit used to attain this result is the central portion of Fig. 1. Tube 1 is operated on the curved part of its characteristic (Fig. 2) and tube 2 is supplied with sufficient plate voltage through a large plate resistance to insure linearity. This linear output is opposite in phase to the output of tube 1 and its magnitude depends on the setting of R_1 and R_2. The outer portions, separated by links, are used for taking characteristics and determining the proper operating points. The two milliammeters and the continuously adjustable grid bias in the amplifier are not essential, but are extremely convenient if many tubes are to be tested. R_s is such that A_2 reads zero when the amplifier plate current equals I_{pp}.

To investigate a particular tube to be used as tube 1 it is first necessary to determine the value of R_{p1} that will give maximum second harmonic output. Now the output will vary directly with $b_2 R_{p1}$ and in Peters' text[1] it is shown that $b_2 = B^2/(1+G_{p1}R_{p1})^3$ where B is a constant of the tube. Differentiating with respect to R_{p1} we find that the maximum output is obtained when $R_{p1} = 1/(2G_{p1})$. This maximum is quite broad and R_{p1} may be made half the manufacturers rated plate resistance without serious loss.

[1] L. J. Peters, Thermionic Vacuum Tube Circuits.

The values of R_1 and R_2 which will bring the vertex of the parabola to a desired operating point may be calculated fairly closely from the tube characteristics, but it is much quicker to use a process of trial and error. The method is to start with (R_2/R_1+R_2) about 0.3, and then with the switch S open, adjust P_1 until the current in A_1 is a minimum. Then adjust P_2 until A_1 reads I_{pp} and close S. The curve, which will resemble those of Fig. 3, can

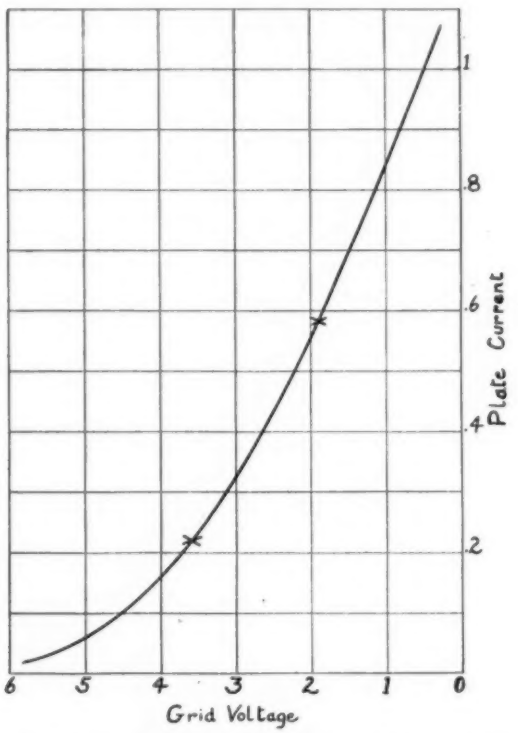

Fig. 2. Grid voltage-plate current characteristic of 201A.

then be plotted. A decrease in R_2 will shift the vertex of the curve toward more negative grid voltages and vice versa. A convenient full scale range for A_2 is 0.2 milliamperes. The current readings are preferably converted to the corresponding grid voltages.

Shape of the Curves

It will soon become apparent that none of these curves are even approximately symmetrical over a very wide range, and this is caused by the fact that (1) is but a poor approximation to the actual shape of the characteristic curve. A closer approximation is $e_{p1}=R_{p1}(b_0+b_1e_g+b_2e_g^2+b_3e_g^3)$ and (2) becomes

$$e_0 = a + R_{p1}b_2e_g^2 + R_{p1}b_3e_g^3. \tag{3}$$

The distortion introduced by the higher order term will be discussed later.

The dissymmetry of this curve (3) is measured by the difference of the

ordinates on the two sides of the curve at a certain grid voltage, and (neglecting terms in e_g^5 etc.) half that difference is the e_g^3 term. Thus in Fig. 3 curve A, $\delta = R_{p1} b_3 e_g^3$.

Since the amplification of the arrangement is of no great importance, the input voltage required to get a certain output does not matter, and the best curve for any tube is the one for which K/M is the greatest. Where K is some

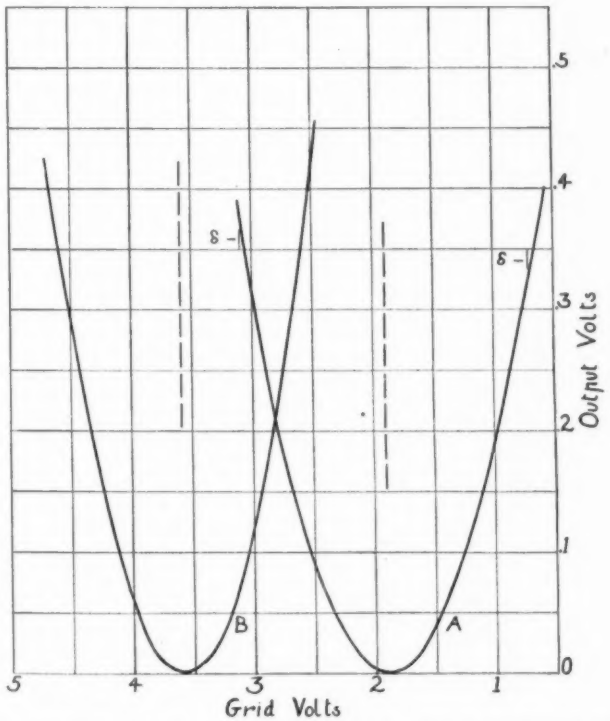

Fig. 3. Input voltage-output voltage characteristic of frequency doubler.

assumed maximum permissible value of δ, and M is the ordinate of the curve at the point where $\delta = K$. Operation at the vertex of this curve will yield the greatest output that is possible without exceeding the permissible distortion. The two curves of Fig. 3 show the relative merits of two operating points for a 201A tube. These points are marked X in Fig. 2 which refers to the same tube. It is interesting to note that b_3 is actually numerically less on the more curved portion of the characteristic. By measurement from curve $3B$ we have

$$e_0 = 0.35 e_g^2 + 0.0085 e_g^3. \tag{4}$$

Distortion

By distortion we may understand, for present purposes, the introduction of either the fundamental frequency or harmonics other than the second in the output. This will be caused either by the presence of a cube term in the equation, by failure to operate at the vertex of the curve, or by both. Let us

investigate the two causes at once by writing the characteristic of the circuit as

$$e_0 = a_2 e_g^2 + a_3 e_g^3 \tag{5}$$

and putting

$$e_g = (k + E \cos \omega t).$$

Substituting and expanding

$$e_0 = \text{constant} + (2a_2 k + 3a_3 k^2 + \tfrac{3}{4} a_3 E^2) E \cos \omega t$$
$$+ \tfrac{1}{2}(a_2 + a_3 k) E^2 \cos 2\omega t + \tfrac{1}{4} a_3 E^3 \cos 3\omega t.$$

Three cases are of interest.

1. If we operate at the vertex, $k = 0$ and

$$e_0 = \tfrac{3}{4} a_3 E^3 \cos \omega t + \tfrac{1}{2} a_2 E^2 \cos 2\omega t + \tfrac{1}{4} a_3 E^3 \cos 3\omega t$$

By using the coefficients from (4) and putting E equal 1 volt we get for the 201A

$$e_0 = 0.0064 \cos \omega t + 0.175 \cos 2\omega t + 0.0021 \cos 3\omega t.$$

The amplitude of the fundamental is 3.6 percent and that of the third harmonic is 1.2 percent of the second harmonic.

2. If $a_3 = 0$ and $k \neq 0$.

$$e_0 = 2a_2 k E \cos \omega t + \tfrac{1}{2} a_2 E^2 \cos 2\omega t.$$

Which gives the amount of fundamental introduced by failure to operate at the vertex.

3. The amplitude of the cos $3\omega t$ term is independent of k, but if we make $k = [-2a_2 \pm (4a_2^2 - 9a_3^2 E^2)^{1/2}]/6a_3$ the coefficient of the cos ωt term becomes zero.

A voltage of fundamental frequency is present in the output due to the grid-plate capacity of the tube. This is negligible at audio-frequencies.

A brief discussion of the results from a different point of view may make their significance clearer. *Case 2.* If

$$e = a_1 e_g + a_2 e_g^2 \tag{1a}$$

represents the characteristic of tube 1 and $e = a_1 e_g$ represents that of tube 2, when we add these in opposite phase in our circuit the resulting characteristic of the combination is

$$e_0 = a_2 e_g^2. \tag{2a}$$

That is to say, we may simply consider that the output of tube 2 just balances out the component of fundamental frequency in the output of tube 1. But if the adjustment is not perfect there will remain a small unbalanced component of fundamental frequency represented by

$$e_0 = \Delta a_1 e_g + a_2 e_g^2. \tag{3a}$$

Now the *shape* of (3a) is exactly the same as (2a), but it is shifted sideways and its vertex is no longer at $e_g = 0$. So again we arrive at the result that failure to operate at the vertex of the curve introduces a component of funda mental frequency in the output.

Case 1. On the other hand the addition of a cubic term to $e_0 = a_2 e_g^2$ giving $e_0 = a_2 e_g^2 + a_3 e_g^3$ does not shift the origin or the vertex of the curve, but simply makes it rise more steeply on one side than on the other. As we have seen, this gives rise to a component of fundamental frequency, and one (a third as large) of third harmonic frequency in the output.

Measurement of Cubic Term in Tube Characteristics

Measurement of the dissymmetry of these curves would appear to be a good direct method of determining the cubic term in the characteristic of a tube, and thence of determining the amount of third harmonic distortion without harmonic analysis of output curves. The greatest source of error in the method is the difficulty of locating exactly the axis of the curves. Probably the best procedure is to locate the axis as nearly as possible by inspection, and then to plot δ (Fig. 3 curve A) against e_g. If the axis was chosen incorrectly this curve will not pass through the origin. A further source of error is curvature in the characteristic of tube 2, which will tend to diminish the dissymmetry.

Representative values of the coefficients a_2 and a_3, (5z are shown in Table I. The plate voltage is 45 in each case.

Table I.

Tube	e_{gp}	a_2	a_3
201A	−3.6	0.35	+0.0085
201A	−1.9	0.25	−0.017
112A	−1.7	0.20	−0.015
112A	−1.1	0.16	−0.014
230	−1.8	0.27	−0.045
230	−1.1	0.17	−0.029

Undoubtedly there are tubes that will give far greater values of a_2/a_3 than the best of these, but the coefficients vary considerably among different tubes of the same type and an investigation of all types of tubes available would not be of general value.

ELECTRON DIFFRACTION FOR CLASSROOM DEMONSTRATION

By C. J. Phillips

Physics Department, Oberlin College

(Received August 17, 1931)

Abstract

An apparatus is described for the class-room demonstration of electron diffraction photographs obtained from thin metallic films and using the range 2000 to 15000 volts. It is very simple to build and reasonably stable. The method of operation is explained.

THE striking phenomena, until quite recently unknown, which occur when high speed electrons are shot through very thin metallic films, must be placed well in the vanguard of the discoveries confirming and fructifying the new wave mechanics.

As is well known, the pattern formed on a photographic plate normal to the electron path consists of an intense central spot due to unscattered electrons, surrounded by a fainter region containing several rings concentric about the central spot. These are due to electrons which have been diffracted in a manner exactly analogous to that of x-rays in a Hull-Debye-Scherrer photograph.

Aside from their purely theoretical interest, these diffraction photographs should prove of instructional and, possibly, industrial use. For class or lecture purposes they would form the most tangible and easily visualized proof of the wave nature of electrons. The form and number of the rings is so closely connected with the type of material used as film and, in particular, is so dependent upon the nature of the film's surface, that it is quite conceivable that electron diffraction may, in the very near future, serve as a valuable method of studying metallic film surfaces.

It seems likely that the greatest deterrent to the application of these uses has been the fact that most of the apparatus so far used has been relatively unstable and not at all uniformly satisfactory in operation.

The apparatus described below, though not particularly novel, is simple to build and operate, is reasonably stable, and furnishes diffraction photographs clear enough to allow optical projection for lecture demonstrations.

Characteristics of the Apparatus

A picture of the completed tube as actually set up is shown in Fig. 1, and a diagrammatic drawing in Fig. 2. Samples of the electron diffraction patterns obtained with this apparatus are shown in Fig. 3. The tube was modeled somewhat after that used by von Kirchner[1] for a similar purpose, but with

[1] Fritz von Kirchner, Phys. Zeits. **31**, 772 (1930).

certain changes and modifications. In Fig. 2, *A* represents the gas discharge tube with glass walls and cathode at *B*. This portion of the tube may, if desired, be made in a quite different shape than that indicated so long as a steady cathode discharge be obtained. The anode is grounded through the brass frame which forms the remainder of the apparatus. A thin-walled brass tube *C*, 13 mm in diameter, runs through the large brass block *D* and is covered at each end by a brass cap which fits snugly over the end of the

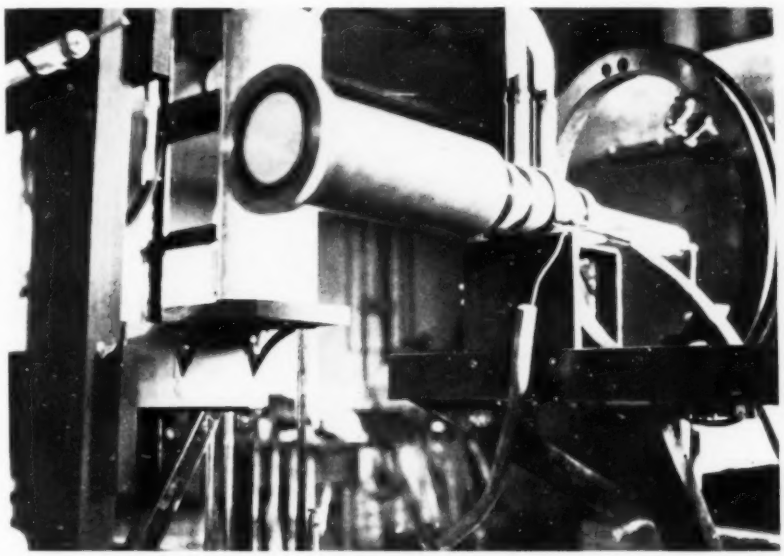

Fig. 1. Photograph of electron diffraction apparatus as set up for laboratory use.

tube. The large brass block makes for extreme rigidity and helps to dissipate any heat that may be generated therein. The cap at *E* contains a very fine hole 0.2 mm in diameter and that at *F* a 0.1 mm hole. Both caps are removable. Over the latter the film is placed, and it is apparent from the drawings that the electron stream must pass through both *E* and *F*. A brass tube *G*, 75 mm in diameter, contains at its lower end an arrangement whereby either a fluorescence screen or a photographic plate may be used to record the diffraction effects. Exhaust tubes *H* and *I* run through a stop-cock directly to the vacuum system. In order that the vacuum may be uniform throughout the whole electron tube, holes *J* and *K* are pierced in the central electron gun *C* and these compensate for any small pressure differences that might arise. This is essential, for the extremely thin film over *F* may otherwise be punctured, particularly if the pumps are fast. All joints and couplings are made vacuum-tight by placing over them rubber gaskets well greased and lying flat against the brass ends as at *O*. These ends contain slight grooves, concentric about the center of the tube, into which the rubber forces itself when the collars *L*, *M*, and *N* are tightened. The position of the first two are only indicated but the construction of the latter, which is typical of all three, is

shown in detail in Fig. 2, together with the method of mounting the photographic plate. When it is desired to use the fluorescence screen, the plate-

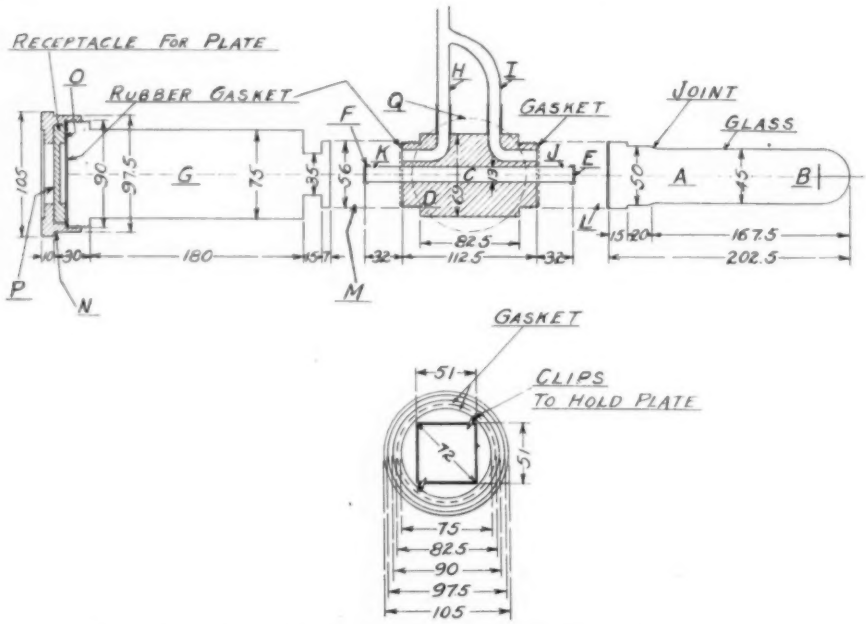

Fig. 2. Diagrammatic drawing of apparatus. All dimensions are in mm.

holder P is simply removed and a ring of equal diameter, containing the screen, is inserted. In order that the stream of electrons may be prevented

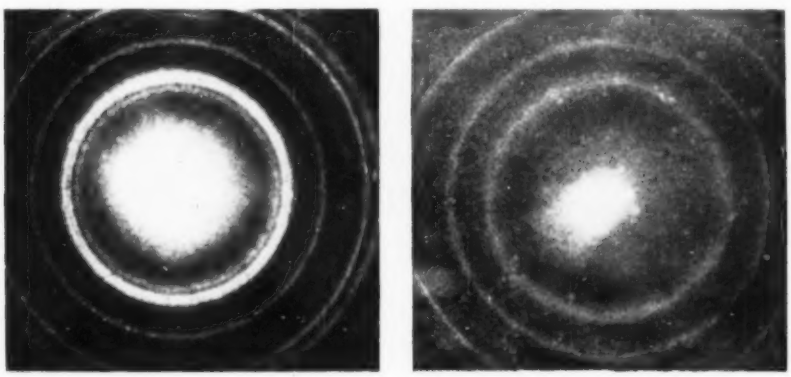

Fig. 3. Samples of electron diffraction patterns.

from going through E and F until needed, a small coil Q was placed at about the center of the tube and a 6 volt current from a storage battery passed directly through it. This deflected the rays until ready for observation.

Films of almost any metal prepared by beating can be used if they are of the order of 10^{-6} cm in thickness. Gold films of this type can be obtained

commercially. These are mounted on the small brass caps by cleaning the latter thoroughly with alcohol, placing a very small quantity of shellac around the hole and pressing the entire cap upon the film. The excess film around the edges can be removed with a sharp knife or razor blade.

Any vacuum system capable of creating and maintaining a pressure sufficiently low for a cathode discharge may be used and the proper time for taking the pictures may be determined by observation of this discharge. Exposure for 15 to 30 seconds has been found to work very well at 4400 volts.

A large induction coil or other similar source of voltage supply may be used and the tube will handle voltages as low as 2000 and as high as 15000, though if the higher voltages are used for more than about 5 minutes at a time the glass around the cathode support may be melted. Several large Leyden jars may be used across the input to steady the discharge.

Mode of Operation

The actual taking of a picture is simple. With the fluorescence screen, and without the film in place, the discharge is centered. If no spot is seen, due to the bending of the electron stream by the earth's magnetic field, that field must be counteracted by a properly placed earth-coil. This is usually an easy matter and when once found the position of the coil can be made permanent. The fluorescence screen is then removed, the film mounted, and evacuation begun. Just before the cathode discharge begins the current in the deflecting coil is turned on. When the proper discharge is being obtained this current is turned off for the time necessary for exposure. The best length of exposure at various voltages can only be obtained by experience.

In conclusion I must acknowledge my indebtedness to Dr. F. G. Tucker of Oberlin college for suggesting this problem, and to Mr. B. J. Smyth, also of Oberlin, for building the necessary apparatus.

THE UNPOLARIZED RESISTIVITY OF GLASS

By Denis M. Robinson, Ph.D.
Massachusetts Institute of Technology
(Received November 7, 1931)

Abstract

An experimental comparison has been made of three methods of measuring the unpolarized resistivity of glass and fused quartz over a temperature range from 20 to 500°C. At high temperatures all three methods are in quantitative agreement and give a straight line when the logarithm of the resistivity is plotted against the reciprocal of the absolute temperature. At lower temperatures, however, the a.c. curve deviates from this straight line, indicating an additional component of loss which does not exist on d.c. This additional loss may be due to the orientation of polar molecules, though no definite proof can be given. The results obtained by the other two methods, both with direct current, are in close agreement over the whole temperature range, and give without doubt the true unpolarized resistivity.

ORDINARY resistance tests on solid dielectrics show a wide divergence from Ohm's law, even at low voltages, and this has been proved to be due to the formation of space charges near one or both electrodes. As the space charge is concentrated in a relatively small thickness the apparent resistivity depends on the thickness of the sample; and due to the time taken in building up the space charge, the resistance varies with the time.

Since the change with time is due to this space-charge effect, the only value of resistivity that has any real significance is the initial or unpolarized value ρ_0, for the value at any other time is dependent on the concentration of charge, which depends on the voltage applied and the thickness. Obviously a value for the "resistivity" which depends on these conditions is of small use.

In the particular case of glass, Buff[1] in 1859 had already noticed the decrease of current with time in glass and explained it as due to increasing polarization. We may here notice that the term is not a good one and it was left to Warburg[2] to make it clear that in glass one ion, that of sodium, is responsible for almost the whole of the conduction, and that the increase of resistivity is brought about by deficiency of sodium ions at the anode leading to a negative space charge in that region. To overcome this Warburg used sodium amalgam as anode, so that fresh sodium was introduced as required into the glass. Under these conditions there was no change with time and he was able to determine the unpolarized resistivity. Instead of using an anode rich in sodium ions Ambronn[3] prevented the formation of space charges by rapidly reversing the direction of the current. Actually he used direct current commutated 200 times a second and measured the current with a mirror galvanom-

[1] Buff, Lieb. Ann. **110**, 257 (1895).
[2] Warburg, Wied. Ann. **21**, 622 (1884); Ann. d. Physik **40**, 327 (1913).
[3] Ambronn, Ann. d. Physik **58**, 139 (1919).

eter before commutation, obtaining the advantage of greater sensitivity than would be given by a dynamometer.

A large amount of work has been done on the general subject of the conductivity of glass and an excellent summary and bibliography of this is given by Fulda.[4]

Although several of these authors have worked on the unpolarized resistivity, they have investigated only one method each, and it has been an open question whether the different methods would give the same result.

Four methods of attack have been suggested:

1. Find the current for a given applied voltage at the initial instant before the space charge can build up.

2. Use of nonpolarizing electrodes. This is the term applied to electrodes which are capable of supplying to the dielectric the type of ions which carry the current in that dielectric.

3. Measurement with alternating voltage. If the field is reversed, the ion migration will be reversed; and it is clear that as the frequency of the applied field is increased a frequency will be reached where, because of the inertia of the ions, they will not move appreciably. The value measured in this way will thus be the unpolarized resistivity.

4. Measurement of the polarization voltage directly. If the electrolytic polarization theory is correct there will be a back e.m.f. which will persist for a short time after the removal of the field. If this voltage P can be measured,

$$\frac{E - P}{I} = R$$

where R is the unpolarized resistance, E is the applied voltage and I is the current at the instant when P is measured.

The objects of the present investigation are to examine the relative feasibility of the first three methods of determining the unpolarized resistivity and to compare quantitatively the values found by each method over the widest possible temperature range, with a few selected materials.

Glass Samples

The following were investigated:

A soda-lime glass made by the Kimble Glass Co.
A lead glass. (Gl)
Pyrex (Laboratory grade) } Cornimg Glass Works.
Fused quartz (Vitrosil), Thermal Syndicate, Ltd.

All were in the form of tubes about 20 cm long, sealed at one end, filled to within about two cm of the top with a liquid electrode and fixed within a larger tube also filled with the liquid electrode to the same height. Up to 250°C mercury was used for both electrodes, and above that temperature soft solder.

[4] Fulda, Sprechsaal (Coburg) **60**, 769 (1927).

The samples were in a well-lagged electric oven, the temperature of which could be varied from room temperature to 500°C. The thermal capacity of the oven was large, so that the temperature variations were slow. The leads were brought out by brass rods supported only by large mica washers. The temperature was measured by means of a Leeds and Northrup platinum resistance thermometer, reading accurately to a tenth of a degree.

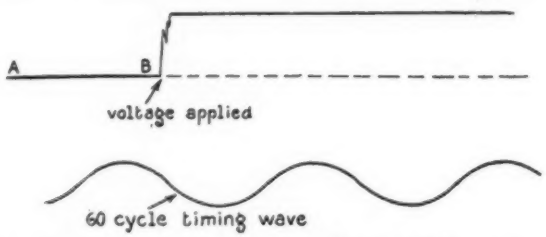

Fig. 1. A typical result for soda-lime glass. (290°C, 24 m.a.).

Apparatus and Methods

The a.c. method

A capacity bridge made by the General Radio Company was used with a head telephone set to measure the resistance of the samples, and a thousand-cycle hummer was used as the a.c. source.

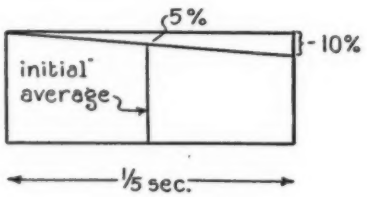

Fig. 2.

Since this bridge became very insensitive at resistances greater than 10^9 ohm, a very sensitive Schering bridge was used for measurements at temperatures below 100°C.

Resistivity from the current at the initial instant

A Westinghouse oscillograph was arranged so that its shutter-operating current was made to close in addition a relay system having a time lag, so that a fraction of a second after the shutter opened, admitting light to the oscillograph, this relay closed the series circuit through the sample.

Fig. 1 shows a typical result for soda-lime glass. AB is the zero axis and its length represents the difference between the lag of the shutter and of the relay system. At B the circuit is closed, and, as seen, the current jumps within one thousandth of a second to its maximum value of about 24 m.a. The amount of overshooting is very slight and there is no evidence of the charging current which is much too small to affect the oscillograph. The decrease of current due to polarization is found to be of the order of 20 percent in half a second.

From this initial current the resistivity may be calculated, but the method has the disadvantage that the resistivity can only be measured at high temperatures when the current is sufficiently great to give a reasonable vibrator deflection. Further, only soda-lime glass has sufficient conductivity with the size of samples and temperature used and an increase of voltage to overcome this may result in breakdown.

The slow rate at which the current decays suggested the possibility of applying the voltage for a short, known interval of time, and measuring the quantity of electricity passed by the sample. For an interval of 1/5th second

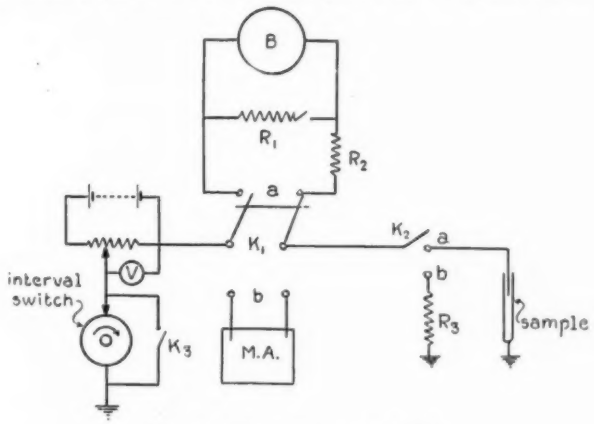

Fig. 3. Arrangement of circuit.

the decrease of current is less than 10 percent and thus the error involved in assuming the average current equals the initial current is less than 5 percent, (Fig. 2), which is sufficiently accurate for our purpose.

This switching was accomplished by using a synchronous motor, driving, through interchangeable gear wheels, a spindle on which was mounted an ebonite bushing having a screw thread of about six turns per inch. A copper wire of exactly one turn lies in the bottom of the last turn of the thread, and a trigger mechanism permits a contact piece to drop into the thread, thus making contact with the copper wire for one revolution. This sliding contact introduced no measurable error as low currents and a high series resistance were employed.

To measure the quantity of electricity passed during this interval a ballistic galvanometer of 1000 ohms resistance was used, shunted when necessary by 100 or 10 ohms. The time of voltage application is accurately known, and the current can be calculated if desired from this and the sensitivity of the ballistic galvanometer.

However, it was found convenient to calibrate the ballistic galvanometer under the conditions of the experiment. This was accomplished by passing a known current, which could be measured in the steady state, through the above described interval switch and ballistic galvanometer. Fig. 3 shows the circuit. R_3 is adjusted so that a suitable current flows through the milliammeter MA when K_3 is closed.

Then with K_3 open and K_1 at a the ballistic galvanometer deflection for the same current through the interval switch can be obtained. R_2 is a compensating resistance equal to the difference of the resistances of MA and B. The current/deflection relation for the ballistic galvanometer was found under these conditions to be perfectly linear, showing the reliability of the time-interval switch.

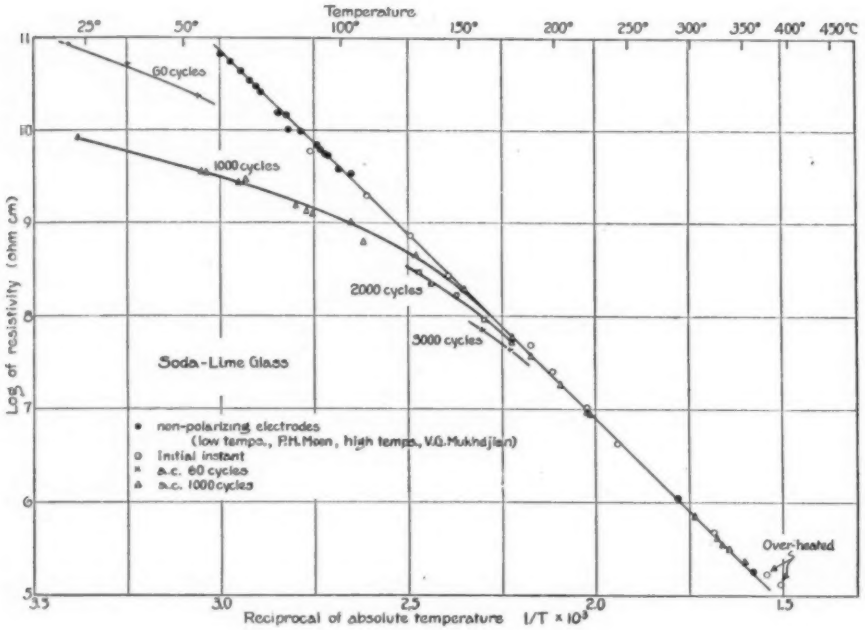

Fig. 4.

Knowing the capacitance of the sample and the applied voltage, the quantity of electricity required to charge the sample electrostatically is determined, and is found to be negligible in comparison with the quantity passed as conduction current during the operation of the switch. As a further check, the gear ratio was altered so that the voltage was applied for 1/12 instead of 1/5 second. No difference larger than the experimental error was observable.

Nonpolarizing electrodes

This method, with sodium nitrite as electrode, has been used by Mukhdjian and Keely[5] with the same four kinds of glass.

The author is indebted to Professor P. H. Moon for permission to include his unpublished results on soda-lime glass with sodium thiosulphate as an electrode.

The samples were from a batch also tested by the other methods.

[5] Schönborn, Zeits. f. Physik **22**, 305 (1924).

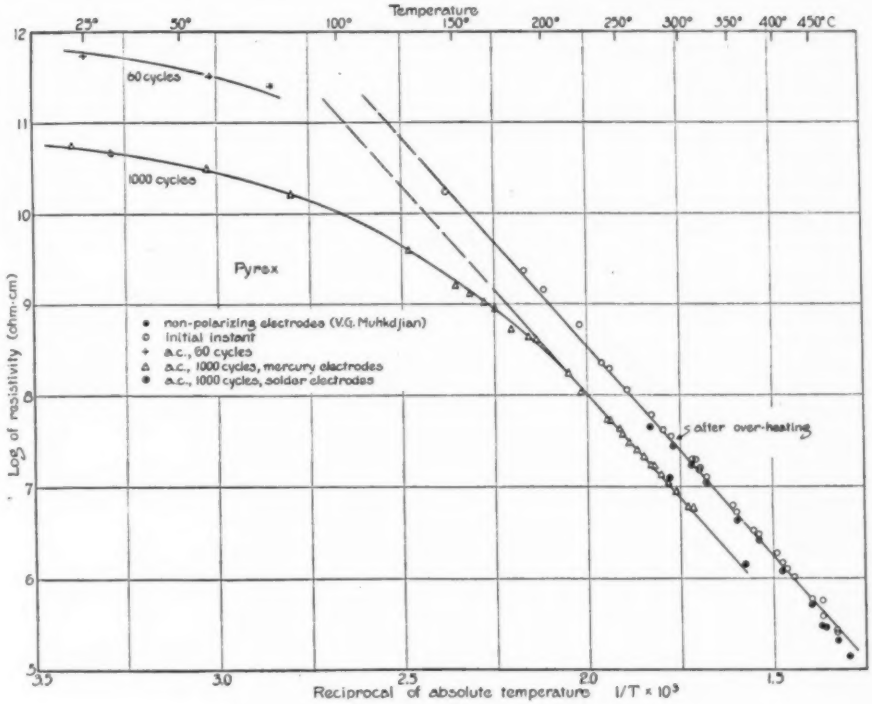
Temperature
25° 50° 100° 150° 200° 250° 300° 350° 400° 450°C
60 cycles
1000 cycles
Pyrex
non-polarizing electrodes (V.G. Mukhdjian)
initial instant
a.c., 60 cycles
a.c., 1000 cycles, mercury electrodes
a.c., 1000 cycles, solder electrodes
after over-heating
Log of resistivity (ohm-cm)
Reciprocal of absolute temperature 1/T × 10³

Fig. 5.

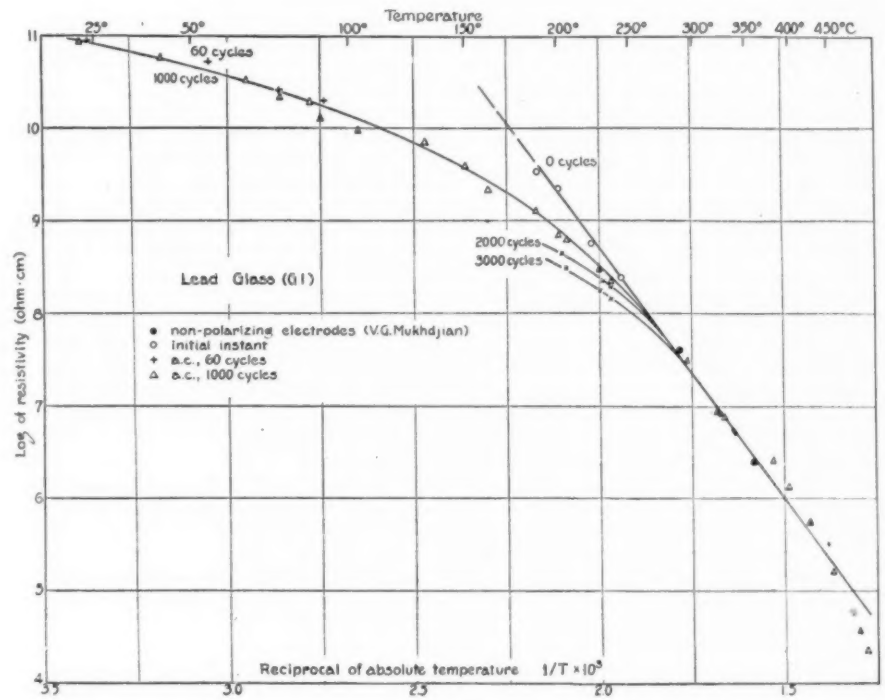
Temperature
25° 50° 100° 150° 200° 250° 300° 350° 400° 450°C
60 cycles
1000 cycles
0 cycles
2000 cycles
3000 cycles
Lead Glass (G1)
non-polarizing electrodes (V.G. Mukhdjian)
initial instant
a.c., 60 cycles
a.c., 1000 cycles
Log of resistivity (ohm-cm)
Reciprocal of absolute temperature 1/T × 10³

Fig. 6.

Results

As the change of resistivity with temperature of a solid dielectric can in general be expressed by

$$\rho = \rho_0 \epsilon^{B/T}$$

the logarithm of the resistivity was plotted against the reciprocal of the absolute temperature to obtain a linear relation. Common logarithms were used for convenience.

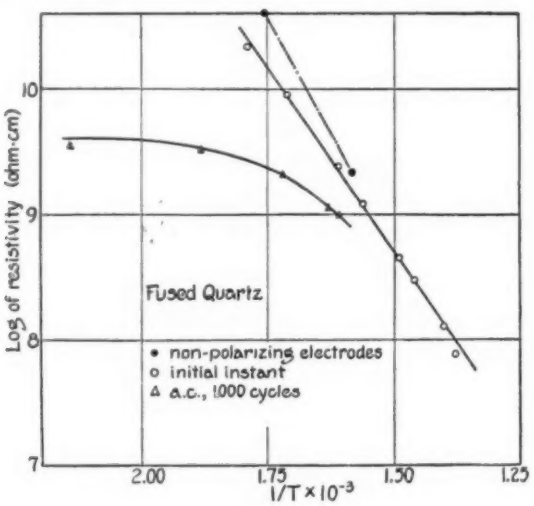

Fig. 7.

Soda-lime glass (Fig. 4)

1. The results for the initial instant agree very closely indeed with those obtained with nonpolarizing electrodes, over the whole range over which they can be compared, i.e., 60°C to 250°C.

2. The two d.c. methods give a straight line on the plot over the whole range of 20°C to 520°C.

3. Between 140°C and 250°C the resistivity as measured with a.c. agrees very closely with the d.c. values.

4. Below 140°C the resistivity as measured with a.c. is much lower, indicating an additional component of loss.

5. This effect increases very remarkably with increase of frequency, both between 60 and 1000 cycles, and between 1000 and 3000 cycles. The higher the frequency the higher is the temperature at which the loss is noticeable.

6. The characteristics of the glass were obviously changed by prolonged heating at high temperatures as shown by the new position of the curve at *a*. However, after this change the initial-instant and a.c. values were still in good agreement. Subsequently a new sample from the same bath was used to continue work on the original curve.

The experimental results for the other samples are similar. (Figs. 4 to 7). It will be noticed that for all four samples the initial-instant results agree

very closely indeed with those obtained with nonpolarizing electrodes. In no case do either initial-instant or nonpolarizing electrode results show any tendency to deviate from the linear relation within the range investigated, i.e., 20°C to 500°C. The slopes of the various curves are given in Table I, which shows a reasonably good agreement between the various methods.

TABLE I. *The value of the constant B in the equation.*

	From the curves	Mukhdjian and Keely
Soda-lime	4000	4250
Pyrex (before heating)	4400	—
(after heating)	4800	4780
Lead glass Gl.	5400	6340
Fused quartz	6000	7040

It will be noted that in all cases the a.c. values at high temperatures also fall upon a straight line. At lower temperatures the a.c. curve bends away from the straight line and falls consistently below it. This shows that in addition to the I^2R loss there is another component of loss on alternating current, though at sufficiently high temperatures the former is so large that it completely masks the latter. The additional loss is evidently a function of both temperature and frequency, and may be explained by either the Debye theory of polar molecules or the Wagner theory of imperfect dielectrics. There seems to be no definite proof of the existence of polar molecules in glasses, and thus the exact nature of this loss is unknown. However, the results of the present investigation show definitely that the a.c. loss cannot be explained on the basis of a pure I^2R loss.

Ambronn[3] using commutated d.c. as already mentioned, found that the resistivity could be accurately predicted at any temperature from the exponential law, except for the lowest temperatures. His numerical results when plotted show at the lowest temperatures the bending over of the curve, and the magnitude of the effect is the same as in the present investigation.

Schönborn[5] found that when a glass was in a state of strain its resistivity changed markedly at about 350°C to 500°C (the annealing zone).

The changes found in this region in the present series of results do not agree with those of Schönborn, but until further work has been done the author hestitates to explain the discrepancy.

EDITOR'S COLUMN

The Isotopes of Hydrogen

THE recently announced discovery[1] of the isotope of hydrogen of atomic number 2 is of very great interest in the theory of the periodic table. The blank interval of two units between hydrogen and helium is a disconcertingly open gap; in filling it in one may be able to obtain new light on the building up of atomic nuclei. The existence of the isotope H^2 has been conjectured[2] before, particularly from the discrepancy between the atomic weight of ordinary hydrogen as determined from chemical data and from Aston's mass spectrograph results.

In the present experiments liquid hydrogen was fractionated by evaporation, the lighter component evaporating more rapidly leaving the residue with an increased concentration of H^2. This residue was then examined spectroscopically for the Balmer lines. The position of the lines depends to some extent on the mass of the nucleus (isotope effect) and the theory shows that one would expect to observe, on the short wavelength side of the Balmer lines of H^1, certain faint lines, the Balmer lines of H^2. On examination such lines were found accompanying the strong lines $H\beta$, $H\gamma$, and $H\delta$ of H^1, agreeing in position within 0.01A with the predicted positions. The $H\alpha$ line of H^2 was not found but the authors state that further work is being done on it. From the relative intensities of the lines the authors estimate that in their residue the concentration of $H^2:H^1 \backsimeq 1:800$, while in ordinary hydrogen the concentration should be about 1:4000, agreeing with the estimate 1:4500 of Birge and Menzel. No evidence of lines for H^3 was found, so that if it exists at all its concentration is very small.

There are many things which one would like to know about H^2: the magnetic moment of the nucleus and the packing fraction are two of the most important. All of these questions must await further work, for as yet only the existence of the isotope has been established.

E. L. HILL

[1] H. C. Urey, F. G. Brickwedde, and G. M. Murphy, New Orleans Meeting of the American Physical Society, Dec. 1931.

[2] Cf. R. T. Birge and D. Menzel, Phys. Rev. **37**, 1669 (1931). Johnston, Journ. Am. Chem. Soc. **53**, 2866 (1931) H. C. Urey, Journ. Am. Chem. Soc. **53**, 2872 (1931).

The Interaction of Light and Matter

THE problem of the interaction of light with matter may be said to be the *pièce de resistance* at the banquet set for the atomic physicists. Parts of it are cut off and apportioned to the workers in the various fields—the γ and cosmic rays,* the x-rays, the ultraviolet, the visible, the infrared, and finally the radio regions are all branches of one and the same study. Generally speaking each field has its own unique problems tying up at certain points with results in neighboring fields but still maintaining its own particular characteristics.

In attempting to develop a unified theory which will cover the phenomena in *all* of these fields at the same time the theorist is perhaps engaged on a quixotic task, but it is nevertheless one which is the more intriguing the more one considers it. It was a development of the first magnitude when Maxwell concluded that light was nought but an electromagnetic wave and that it should be governed by his famous equations. At that time the word "light" referred principally to the visible region and to the region on the

* The evidence is not clear as yet as to whether or not cosmic rays are photons, electrons, or perhaps neutrons. Cf. J. F. Carlson and J. R. Oppenheimer, New Orleans Meeting of the *American Physical Society*, Dec. 1931.

long wave-length side of the visible. X-rays, not to speak of cosmic rays, were still in the womb of time. Under the impetus of Maxwell's theory the problem of light was at once definitely divided into two parts, a division which has exerted a profound influence on the whole subsequent development of the subject. That is, one spoke of the propagation of light in "free" space on the one hand, and of the propagation of light in "ponderable" bodies on the other. Light thus came really to have an existence independent of matter although it could be "created" and "destroyed" through the influence of matter. And this in spite of the fact that light is never apparent as such but only through its interaction with matter; an invisible messenger from distant regions whose presence is not even suspected until it has delivered its message.

For the propagation of light in "free" space Maxwell's original theory is valid to this day. It is in the vitally important question of the mode of interaction of light and matter that doubt and indecision have arisen. Maxwell's answer to this problem was characteristic of the physics of his day. The propagation of light in ponderable media was treated in much the same manner as for empty space except that one introduced certain material "constants" characteristic of the medium: the dielectric constant and the magnetic permeability. These characteristic constants were to be determined experimentally. In addition one set down certain conditions to be satisfied at the boundaries between media and between a medium and free space—the boundary conditions. This constituted the tools by means of which all questions of reflection, refraction, and propagation were to be handled. While this procedure was of a very formal nature the results were remarkably in agreement with experiment within the range of long wave-lengths, and Maxwell's theory will always remain as a supreme accomplishment of ninteenth century physics.

This theory was later amplified by Larmor, Lorentz, and others to include such observed phenomena as dispersion, the normal Zeeman effect, etc. In this process some account had to be taken of the "fine-structure" of the medium, and the presence of a molecular structure began gradually to make its presence felt.

WITH the advent and development of atomic physics, however, new ideas have been developed applicable to the phenomena which are observed in the region of very short wave-lengths. The photon or light quantum has become a definite feature of physical theory, even though there are still difficulties in adopting it into the quantum theory of light as has been mentioned in these columns before.[1] Even if we do not directly adopt the extreme light quantum hypothesis, still the evidence of spectroscopy teaches us that light is absorbed or emitted by single atoms or molecules in definite energy units. The quantum theory of light initiated by Dirac[1] has been concerned principally with the interaction of light with single atoms or molecules. How is one to reconcile this with the formal features of the classical theory—with dielectric constants, magnetic permeabilities, and above all with boundary conditions?

Clearly these are statistical quantities referring to *collections* or *aggregates* of atoms. The treatment of dielectric constants and magnetic permeabilities for matter in the bulk is standard and well known to every student of electromagnetic theory. Considering that one can look upon the atoms in a solid as being independent, to a first approximation, and as possessed of individual electric and magnetic moments, one can find the *average* electric or magnetic moment per unit volume of the substance and so can find the dielectric and magnetic constants of the medium. These values can then be inserted directly into Maxwell's equations for the propagation of light. This extension of the theory then enables one to calculate the constants which enter in Maxwell's theory in terms of the molecular structure of the medium; and one gets a semi-classical theory combining the advantages of the formal theory of Maxwell with some of the modernity of quantum physics which has been used with great effect in the discussion of numerous problems.[2]

---

[1] Editor's Column, Physics **1**, 208 (1931).

[2] M. Born, "Dynamik der Kristallgitter," Leipzig (1915).

P. Ewald "Die Reflexion and Brechung des Lichts als Problem der Elektronintheorie" Berlin (1925).

M. Born and O. F. Bollnow, Handbuch

This method is, however, still not satisfactory if one desires to think of the propagation of light in liquids or solids directly on the basis of the concepts applicable to the interaction of light with *individual atomic systems*. By giving up the formal part of the theory which is the strong feature of Maxwell's method the problem becomes much more difficult and one faces a whole host of formidable questions. What is the substitute for the boundary conditions? What is the mechanism by which the light is transferred from one part of the medium to another part?

Preliminary steps in the development of such a theory have been taken by Frenkel[3] in two papers in the Physical Review. This theory is based upon the idea, already used to some extent in other fields, that a solid body; i.e., a crystal, is analogous to a gigantic molecule, so that it is really a single gargantuan system governed by the laws of quantum mechanics. One must then treat it by the known methods of quantum mechanics. Still, the problem is of great difficulty, since one can't by any manner of means solve exactly the problem of determining the allowed quantum states of such a complicated system; the best one can do is to use some kind of approximation or "perturbation" scheme. If one imagines a lattice made up of a series of relatively isolated atoms all of the same kind, then one can imagine a process in which the first atom absorbs a quantum of light and becomes excited. In the next step this atom becomes de-excited and one of its neighbors becomes excited. This transfer continues from atom to atom, a situation which one can describe by saying that the "excitation state" travels from atom to atom. This is the simple picture. The next degree of complexity is to consider that the proximity of the atoms causes a stronger coupling between them so that they are only semi-independent. Their energy levels become disturbed, being slightly shifted and broken up to form a "multiplet." The absorption frequencies of the solid are thus no longer the same as the absorption frequencies of the individual atoms, but are formed into bands of closely spaced absorption lines, as discussed by Breit and Salant[3] in their treatment of the Raman frequencies observed in the scattering of light by liquids. Instead of treating of a *single* excitation state as being transmitted from atom to atom one can build up excitation "waves" or "packets" to describe the superposition of several excitation states. These new excitation states are states in which the energy is no longer located in a single atom, but instead is distributed over a region of the crystal.

In addition to the excitation of the electronic levels of the constituent atoms, one must also consider that the atoms can vibrate as do the component atoms in a molecule. There is then a certain chance that the energy which is stored in the excited electronic levels of the atoms will be transferred into vibrational energy. This vibrational motion is just that which is ordinarily associated with the "heat motion" of the atoms in the lattice. Proceeding in this manner Frenkel calculates the rate at which the light energy will be transferred into heat motion in the crystal via excitation of the electronic levels of the atoms. For extended details of the theory the original papers should be consulted.

These ideas bring to mind many questions of a very interesting nature. In this theory one sees that "light" as such plays an entirely insignificant rôle, merely serving to excite a few of the atoms, the *energy* or *excitation*, as one wishes to think of it, being then passed on from atom to atom. One wonders if it might not be possible to develop a theory in which light did not appear as an element, but only that "excitation states" are passed from one atom to another even though they be separated by large distances. Such questions as these bring forcibly to mind the dictum that to settle one question in physics is to raise a hundred others! The further one looks into Nature the more there is to see.

E. L. HILL

der Physik, Band 24. These references contain citations to other books and to the original literature.

[3] J. Frenkel, Phys. Rev. **37**, 17 and 1276 (1931). See also G. Breit and E. O. Salant, Phys. Rev. **36**, 871 (1930).